Crystallographic Investigation of the Inhibition Mode of a VIM-2 Metallo-β-lactamase from *Pseudomonas aeruginosa* by a Mercaptocarboxylate Inhibitor

Yoshihiro Yamaguchi,*,§,⊥ Wanchun Jin,‡ Kazuyo Matsunaga,‡ Shinnji Ikemizu,¶ Yuriko Yamagata,¶ Jun-ichi Wachino,† Naohiro Shibata,† Yoshichika Arakawa,† and Hiromasa Kurosaki*,‡,⊥

Environmental Safety Center, Kumamoto University, 39-1 Kurokami 2-Chome, Kumamoto 860-8555, Japan, Departments of Structure-Function Physical Chemistry and Structural Biology, Graduate School of Pharmaceutical Sciences, Kumamoto University, Oe-honmachi 5-1, Kumamoto 862-0973, Japan, and Department of Bacterial Pathogenesis and Infection Control, National Institute of Infectious Diseases, 4-7-1 Gakuen, Musashi-Murayama, Tokyo 208-0011, Japan

Received August 19, 2007

The VIM-2 metallo-β-lactamase enzyme from *Pseudomonas aeruginosa* catalyzes the hydrolysis of most β-lactam antibiotics including carbapenems, and there are currently no potent inhibitors of such enzymes. We found *rac*-2-ω-phenylpropyl-3-mercaptopropionic acid, phenylC3SH, to be a potent inhibitor of VIM-2. The structure of the VIM-2−phenylC3SH complex was determined by X-ray crystallography to 2.3 Å. The structure revealed that the thiol group of phenylC3SH bridged to the two zinc(II) ions and the phenyl group interacted with Tyr67(47) on loop1 near the active site, by π−π stacking interactions. The methylene group interacted with Phe61(42) located at the bottom of loop1 through CH−π interactions. Dynamic movements were observed in Arg228(185) and Asn233(190) on loop2, compared with the native structure (PDB code: 1KO3). These results suggest that the above-mentioned four residues play important roles in the binding and recognition of inhibitors or substrates and in stabilizing a loop in the VIM-2 enzyme.

Introduction

β-Lactamases catalyze the hydrolysis of the C−N bond of the β-lactam ring in β-lactam antibiotics, rendering them inactive.[1,2] In the family of β-lactamases, four molecular classes, A−D, were defined on the basis of their amino acid sequence homologies.[3−5] Classes A, C, and D are serine β-lactamases containing a serine residue at the active site, whereas class B metallo-β-lactamases (MBLs[a]) contain one or two zinc(II) ions at the active site. Moreover, MBLs are classified into three subclasses:[6,7] subclass B1 including BcII,[8] an IMP family (IMP-1 to IMP-18),[9] CcrA,[10] and a VIM family (VIM-1 to VIM-11a and -11b);[9] subclass B2 including CphA[11] and ImiS;[12] and subclass B3 including L1[13] and THIN-B.[14] Of all the MBLs, the VIM family and the IMP family are emerging as a worldwide source of acquired carbapenem resistance among Gram-negative bacteria. In variants of VIMs, VIM-2 was first detected from *Pseudomonas aeruginosa* in France in 1996[15] and is now one of the most widespread enzymes in well-known MBLs. The VIM-2 enzyme shows a 24–31% identity with other subclass B1 MBLs such as BlaB, CcrA, and IMP-1.[15]

The bla_{VIM-2} gene is located in a mobile plasmid-encoded gene cassette inserted into the variable region of an integron structure so that horizontal spread of resistance is possible. In fact, bla_{VIM-2} genes have been detected mostly in the Mediterranean countries of Europe, in the Far East regions, including Japan, and at present, in American regions, including the U.S., whereas bla_{IMP-1} genes were first detected mainly in Japan and subsequently isolated in Asia, Europe, and South America.[9] Moreover, in addition to the high resistance against β-lactam antibiotics, there are no clinically available inhibitors for the VIM-2 enzyme including other MBLs at present. Thus, the development of inhibitors is an important subject. The active site in an MBL is made up of the zinc(II) ion(s), the zinc(II) ion binding residues, and two loops. In the two loops, the first loop (loop1) is composed of two β-sheets and a turn constitutes a β-sheet flap, whereas the second loop (loop2) is approximately positioned in the opposite site of loop1 centered about the zinc(II) ion binding site. It is thought that these loops are responsible for substrate recognition, binding, and catalysis in MBLs.[16−22]

To develop potent and common inhibitors, it is necessary to focus on the structure and dynamics of both the zinc(II) ion binding site and loops 1 and 2 in each MBL and its complex with a lead compound.

So far, X-ray crystal structures of MBLs complexed with various inhibitors have been reported with the exception of the VIM-2 enzyme: CcrA−4-morpholineethanesulfonic acid,[23] CcrA−biphenyltetrazoles,[24] IMP-1−mercaptocarboxylate derivative,[22] IMP-1−2,3-disubstituted succinic acid derivatives,[25] IMP-1−irreversible thiol compound with a good leaving group,[26] IMP-1−dansylC4SH,[27] BlaB−D-captopril,[28] and FEZ−D-captopril.[29]

In VIM-2, in 2001, García-Sáez et al. deposited two X-ray crystal structures of VIM-2 in the reduced (denoted as the native VIM-2 enzyme) and oxidized forms of Cys221(178) from *P. aerginosa* into the Protein Data Bank (PDB codes 1KO2 and 1KO3). As far as we know, however, detailed information on the structure of the VIM-2 enzyme complexed with an inhibitor is not available.

* To whom correspondence should be addressed. For Y.Y.: phone, +81-96-342-3238; fax, +81-96-342-3237; e-mail, yyamagu@gpo.kumamoto-u.ac.jp. For H.K.: phone and fax, +81-96-371-4314; e-mail, ayasaya@gpo.kumamoto-u.ac.jp.

§ Environmental Safety Center, Kumamoto University.

⊥ These authors contributed equally to work.

‡ Department of Structure-Function Physical Chemistry, Kumamoto University.

¶ Department of Structural Biology, Kumamoto University.

† National Institute of Infectious Diseases.

[a] Abbreviations: BBL, class B β-lactamase; MAD, multiwavelength anomalous dispersion; MBLs, metallo-β-lactamases; PEG MME5000, polyethylene glycol monomethyl ether 5000; phenylC3SH, 2-ω-phenylpropyl-3-mercaptopropionic acid. In this paper, the amino acid residues of metallo-β-lactamase are designated with the BBL number and the amino acid sequence number by putting the latter in parentheses.

10.1021/jm701031n CCC: $37.00
Published on Web 12/06/2007

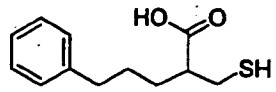

PhenylC3SH

Figure 1. Structure of *rac*-2-ω-phenylpropyl-3-mercaptopropionic acid, phenylC3SH.

We are currently in the process of synthesizing several inhibitors and screening them for inhibitory activity against the VIM-2 and IMP-1 enzymes for the purpose of developing inhibitors for MBLs. In this process, the mercaptocarboxylate inhibitor, PhenylC3SH (Figure 1), was found to be a potent inhibitor of the VIM-2 enzyme with a K_i value of 220 nM, whereas it is less active for the IMP-1 enzyme (K_i = 1660 nM).[30]

For the purpose of understanding structure–activity relationships of the VIM-2 enzyme with respect to phenylC3SH, we carried out X-ray crystallography of the VIM-2 enzyme complexed with phenylC3SH.

Here, we report on the X-ray crystal structure of the VIM-2 enzyme from *P. aeruginosa* complexed with phenylC3SH determined at a resolution of 2.3 Å.

Results and Discussion

In this study, we determined the crystal structure of the VIM-2 enzyme complexed with phenylC3SH in order to elucidate the detailed binding mode of the inhibitor with the enzyme, in particular, focusing on the role of the mobile loop, along with a comparison of the native VIM-2 structure (PDB code 1KO3).

Overall Structure of the VIM-2 Enzyme Complexed with PhenylC3SH. The final refined structural model contained two VIM-2−phenylC3SH molecules in an asymmetric unit, consisting of Glu30(12)−Val290(236) residue each for molecules A and B. The root-mean-squared deviation (rmsd) value between the α-carbon atoms of the two monomers was about 0.28 Å. In molecules A and B, two zinc(II) ions and one phenylC3SH molecule are located at the active sites. The final $R_{working}$ and R_{free} values were 0.212 and 0.247, respectively, and the rmsd values from ideal bond distances and angles were 0.007 Å and 2.0°, respectively (Table 1). The overall structure of the inhibitor complex adopts an αβ/βα sandwich structure, where the active site containing the two zinc(II) ions is located at the bottom at the interface of the two β-sheets surrounded by two α-helices, which resemble those of other subclass B1 MBLs.[22,28,31]

In addition, a clear electron density corresponding to a phenylC3SH molecule was found in the active center (Figures 2 and 3). Although the crystals were grown in the presence of a racemic mixture of phenylC3SH, only the *S*-isomer of the inhibitor was observed in the complex.

All main chain dihedral angles were within the allowed regions of a Ramachandran plot except Asp84(64) and Ala195(158) which adopted φ, ψ angles of 73/74° (molecules A/B), 151/149°, and −151/−157°, −106/−106°, respectively. Asp84(64) is buried in the protein, whereas Ala195(158) is positioned on top of a hairpin loop formed from Tyr191(154)−Val202(165). Asp84(64) and Ala195(158) have strained main chain conformations in both the native VIM-2 enzyme and the phenylC3SH complex. In the crystal structures of BcII, CcrA, and IMP-1 metallo-β-lactamases,[22,31,32] Asp84s were found to have a common strained conformation. Therefore, the conservation of the conformation of Asp84 suggests that it is important for the folding of metallo-β-lactamases. In additional supporting evidence, tRNA maturase RNase Z (PDB code 1Y44)[33] and pre-mRNA 3′-end-processing endonuclease CPSF-73 (PDB code 2I7T)[34] in the metallo-β-lactamase family also have strained main chain conformations of the Asp residues, as has been found for Asp84 of MBLs.

The structures of molecule A in an asymmetric unit of the phenylC3SH complex and that of the native VIM-2 enzyme (PDB code 1KO3) are superimposable except for residues Lys291(237)−Asn295(241), and the rmsd for the α-carbon atoms between them was 0.56 Å. In a comparison of the deviations of the α-carbon atoms between each of the amino acid residues of the native VIM-2 enzyme and the inhibitor complex, residues that moved more than 1 Å were Val34(16) (1.4 Å), Ser35(17) (2.7 Å), Glu36(18) (2.3 Å), Ile37(19) (1.0 Å), Pro38(20) (1.2 Å), Val39(21) (1.1 Å), Ser60(41) (1.5 Å), Phe61(42) (1.8 Å), Asp62(43) (1.9 Å), Gly63(44) (2.0 Å), Ala64(45) (1.4 Å), Val66(46) (1.2 Å), and Gly232(189) (1.8 Å), respectively.

Of these residues, Val34(16), Ser35(17), Glu36(18), Ile37(19), Pro38(20), and Val39(21) were located at the N terminus and Ser60(41), Phe61(42), Asp62(43), Gly63(44) (2.3 Å), Ala64(45), and Val66(46) were located on loop1, whereas Gly232(189) was located on loop2.

Active Site of the VIM-2 Enzyme Complexed with PhenylC3SH. In the phenylC3SH complex, one of two zinc(II) ions (Zn1) was coordinated to His116(94), His118(96), and His196(159) residues with distances of 2.2/2.1 Å (in molecules A/B), 2.0/2.2 Å, and 2.2/2.2 Å, respectively.

The thiol group of the inhibitor is bridged to the two zinc(II) ions (the distances of Zn1−S and Zn2−S were 2.5/2.2 Å and 2.1/2.2 Å), respectively, forming a tetrahedral coordination around the Zn1 atom (the average angle of ligand−Zn1−ligand is 109° for molecule A and 110° for molecule B; Figure 3, Table 2). The coordination of the thiol group of an inhibitor to two zinc(II) ions is similar to those found in IMP-1 complexed with 2-[5-(1-tetrazoylmethyl)thien-3-yl]-*N*-[2-(mercaptomethyl)-4-(phenylbutyrylglycine)][22] or with dansylC4SH[27] and in BlaB complexed with D-captopril.[28]

The second zinc(II) ion (Zn2) is also tetrahedrally coordinated by Asp120(98), Cys221(178), and His263(220) residues, and the thiol group of the inhibitor with distances of 1.9/2.0, 2.2/2.2, 2.1/2.1, and 2.1/2.2 Å, respectively (the average angles of ligand−Zn2−ligand is 109° for molecules A and B, respectively; Figure 3, Table 2). The Zn1−Zn2 distance is 3.8 Å for molecule A and 3.7 Å for molecule B, and this distance is close to those found in the IMP-1 and BlaB enzymes in complex with an inhibitor containing a thiol group (the average distance of 3.6–3.7 Å).[22,27,28]

In the native VIM-2 structure, the geometry around the Zn1 atom is a distorted tetrahedral with three His residues (His116(94), His118(96), and His196(159)) and H_2O/or OH^- (this H_2O/or OH^- is thought to act as the attacking nucleophile on the carbonyl carbon atom of the β-lactam ring),[31,35,36] bridging to the Zn1 and Zn2 atoms, whereas that around the Zn2 atom is a distorted square-pyramid with the basal plane defined by a H_2O/or OH^-, Asp120(98), Cys221(178), His263(220), and Cl atom, where the Cl atom interacts weakly with the Zn2 atom with a distance of 2.9 Å. The apical position is occupied by Asp120(98). In the crystal structures of other subclass B1 MBLs (CcrA and IMP-1),[22,31] the Cl atom in the Zn2 site of the native VIM-2 enzyme is replaced by H_2O, which is thought to contribute to the catalysis of the hydrolysis of β-lactam antibiotics.[31,37] Unlike the native VIM-2 enzyme, the coordination geometry around the Zn2 atom in CcrA and IMP-1 is a distorted trigonal bipyramid.

Table 1. Crystallographic Data Collection and Refinement Statistics for the VIM-2 Enzyme Complexed with PhenylC3SH

data collection				
data set wavelength (Å)	1.0000 (final)	1.2826 (edge)	1.2817 (peak)	1.2906 (remote)
resolution (outer shell) (Å)	50.0–2.30 (2.38–2.30)	99.0–2.53 (2.63–2.53)	99.0–2.54 (2.63–2.54)	99.0–2.55 (2.65–2.55)
cell dimensions				
a, *b*, and *c* (Å)	45.2, 90.75, 129.0			
space group	$P2_12_12_1$			
molecules/asymmetric unit	2			
completeness (outer shell) (%)	99.6 (98.4)	99.2 (96.3)	99.1 (96.7)	99.0 (94.8)
R_{merge}[a] (outer shell)	0.062 (0.267)	0.047 (0.106)	0.050 (0.097)	0.046 (0.121)
no. of observed reflns	163206	123781	122809	121255
no. of unique reflns	24156	18155	18121	17742
$\langle I/(\sigma)\rangle$ (outer shell)	34.9 (4.45)	54.2 (25.5)	55.5 (30.1)	53.4 (23.3)
refinement statistics				
resolution (Å)	42.8–2.30			
no. of non-H atoms[b]				
protein	3392			
ligand	50			
water	212			
rmsd from ideal[c]				
bond length (Å)	0.007			
angles (deg)	2.0			
$R_{working}$[d]	0.212			
R_{free}[e]	0.247			

[a] $R_{merge} = \sum|I_j - \langle I_j\rangle|/\sum I_j$, where I_j is the observed intensity for reflection j and $\langle I_j\rangle$ is the average intensity calculated for reflection j from replicate data. [b] Per asymmetric unit. [c] rmsd: root-mean-square-deviation. [d] $R_{working} = \sum||F_o| - |F_c||/\sum|F_o|$, where F_o and F_c are the observed and calculated structure factors, respectively. [e] $R_{free} = \sum||F_o| - |F_c||/\sum|F_o|$ for 5% of the data not used at any stage of structural refinement.

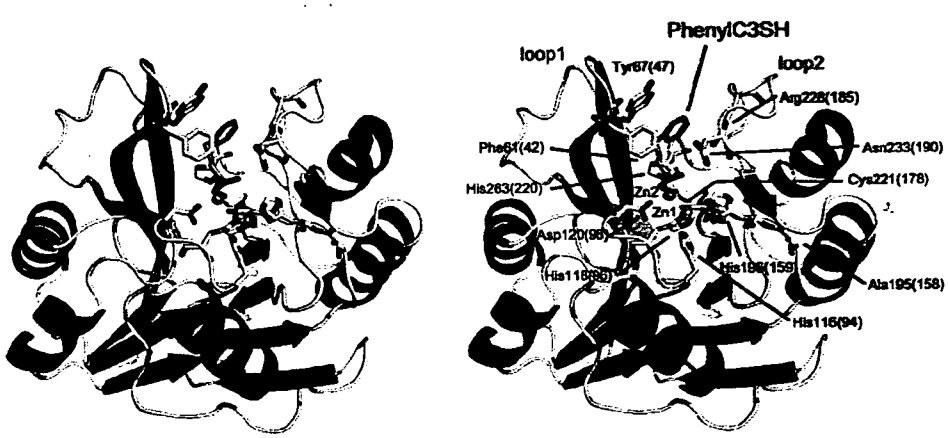

Figure 2. Overall structure of the VIM-2 enzyme from *P. aerginosa* is complexed with phenylC3SH. Molecule A of the phenylC3SH complex is depicted, and the amino acid residues of VIM-2 are designated by a BBL number and an amino acid sequence number; the latter is in parentheses. α-Helices, β-strands, and loops are shown in red, green, and yellow, respectively. Zn(II) atoms are shown as orange spheres. Carbon, oxygen, and sulfur atoms in phenylC3SH are shown as magenta, red, and light-green sticks, respectively. The figure was prepared with PyMol software (http://pymol.sourceforgen.net/).

Comparison of Loop between the Native VIM-2 Enzyme and the PhenylC3SH Complex. The VIM-2 enzyme contains loop1 (Phe61(42)−Ala64(45)) and loop2 (Ile223(180)−Trp242(199)).

Upon inhibitor binding, significant structural changes were found in both loops. The amino acid residues on loop1 are thought to be the most important for substrate recognition and binding, catalysis, and inhibition.[16–19,22] In the phenylC3SH complex, Tyr67(47) and Phe61(42), located on loop1, moved toward the active site to facilitate the interaction with the inhibitor (Figure 4). Compared to the native VIM-2 structure, Tyr67(47) rotates by ~27° about the Cβ−Cγ bond of Tyr67(47) to provide face-to-face π−π stacking interactions between the phenyl rings of the inhibitor and Tyr67(47) with spacing planes of ~3.6 Å (Figures 3 and 4). At the same time, the phenyl ring of Phe61(42) lie ~1.3 Å closer to Zn2 (Figure 4), forming CH−π interactions with the methylene chain of the inhibitor, and these interactions may contribute to the stabilization of loop1. In addition, the active site of the phenylC3SH complex is transformed from an opened cavity into a tunnel-shaped cavity upon binding of an inhibitor (Figure 5).

In loop2 of the phenylC3SH complex, the carboxyl group (O2) of the inhibitor interacts through a hydrogen bond with the side chain ND2 of Asn233(190) (2.9/2.6 Å in molecules A/B), which is conserved in most MBLs.[36] A comparison of the structures between the native VIM-2 and the inhibitor complex showed that conformational change in Asn233(190) is accomplished by the rotation of the neighboring amino acid Gly232(189) (φ and ψ angles are −85° and −119°, respectively, for the native VIM-2 enzyme, whereas those of the phenylC3SH complex are 73° and −143° for molecule A and 63° and −143° for molecule B, respectively; Figure 4). In addition, the binding of the inhibitor to the active site triggers a conformational change in the side chain Arg228(185) (Figure 4): the torsion angle of CB−CG−CD−NE of Arg228(185) is changed from −48° in the native VIM-2 enzyme to 172° for molecule A and −175° for molecule B, respectively, in the phenylC3SH complex. These results suggest that Phe61(42), Tyr67(47), Arg228(185), and Asn233(190) are functionally important residues that play roles in the binding and recognition of the inhibitor or substrate and in stabilizing loops 1 and 2.

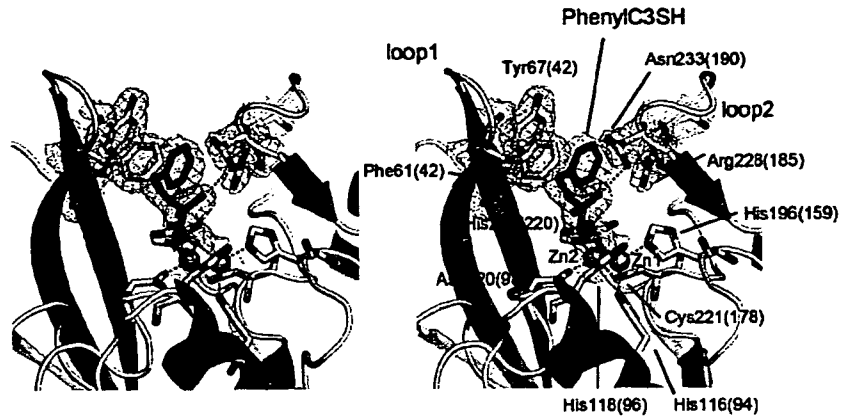

Figure 3. Stereoview of the active site of the VIM-2 enzyme complexed with phenylC3SH. Molecule A of the phenylC3SH complex is depicted, and the amino acid residues of VIM-2 are labeled with a BBL number and an amino acid sequence number; the latter is in parentheses. The electron density map (pink mesh) of phenylC3SH is shown contoured at the 1.0σ level in the $2|F_o| - |F_c|$ map. Zn(II) atoms are shown as orange spheres. Phe61(42), Tyr67(47), His116(94), His118(96), His196(159), His263(220), Asp120(98), Cys221(178), Arg228(185), and Asn233(190) residues and phenylC3SH are represented as sticks. Carbon atoms in amino acid residues are shown in gray (nitrogen, blue; oxygen, red; and sulfur, light-green), and carbon atoms in phenylC3SH are shown in magenta (oxygen, red; sulfur, light-green). The figure was prepared with PyMol software (http://pymol.sourceforgen.net/).

Table 2. Zinc(II)−Ligand Distances (Å) and Angles (deg) for the Native VIM-2 Enzyme and the PhenylC3SH Complex

		distance	
Zn(II)−ligand		native VIM-2	VIM-2−phenylC3SH complex[a]
Zn1	His116(94)NE2	2.2	2.0/2.1
	His118(96)ND1	2.1	2.0/2.2
	His196(159)NE2	2.2	2.2/2.2
	O(w)	2.1	
	S(phenylC3SH)		2.5/2.2
Zn2	Asp120(98)OD2	2.3	1.9/2.0
	Cys221(178)SG	2.3	2.2/2.2
	His263(220)NE2	2.3	2.1/2.1
	O(w)	2.5	
	S(phenylC3SH)		2.1/2.2
	Cl	2.9	
Zn1	Zn2	4.2	3.8/3.7

			angle	
ligand−Zn(II)−ligand			native VIM-2	VIM-2−phenylC3SH complex[a]
His116(94)NE2	Zn1	His118(96)ND1	103	105/105
	Zn1	His196(96)NE2	103	120/110
	Zn1	O(w)	103	
	Zn1	S(inhibitor)		116/126
His118(96)ND1	Zn1	His196(159)NE2	116	101/107
	Zn1	O(w)	119	
	Zn1	S(inhibitor)		113/112
His196(159)NE2	Zn1	O(w)	111	
	Zn1	S(inhibitor)		101/97
Asp120(98)OD2	Zn2	Cys221(178)SG	103	114/117
	Zn2	His263(220)NE2	94	96/99
	Zn2	O(w)	74	
	Zn2	S(inhibitor)		100/100
	Zn	Cl	101	
Cys221(178)SG	Zn2	His263(220)NE2	103	104/105
	Zn2	O(w)	98	
	Zn2	S(inhibitor)		124/116
	Zn2	Cl	152	
His263(220)NE2	Zn2	O(w)	157	
	Zn2	S(inhibitor)		116/119
	Zn2	Cl	103	

[a] The distances and angles for the phenylC3SH complex are quoted for molecules A and B in the asymmetric unit.

Comparison of Loops 1 and 2 between the IMP-1 and VIM-2 Enzymes. We compared the amino acid residues on loops 1 and 2 between the VIM-2 and IMP-1 enzymes (Figure 6). In the case of the IMP-1 enzyme,[22] Trp64(28) is located on the top of loop1, and this residue is thought to be important for the binding of both inhibitors and substrates. Indeed, the role of Trp64(28) in the binding of inhibitors has been demonstrated in X-ray crystal structures of the IMP-1−mercaptocarboxylate inhibitor and −dansylC4SH complexes; the indole ring of Tyr64(28) interacts with the aromatic ring of the inhibitor, and this interaction causes a dynamic movement of loop1 to cover an inhibitor into the active site.[22,27] On the other hand, Trp64(28) in the IMP-1 enzyme is replaced with Ala64(45) in the VIM-2 enzyme. Therefore, in the VIM-2 enzyme, Trp64(28) in IMP-1 is covered with the hydrophobic residues Phe61(42) and Tyr67(47) located in the root of the loop1. Phe61(42) and Tyr67(47) in the VIM-2 enzyme are replaced by Val61(25) and Val67(31), respectively, in the IMP-1 enzyme. It is thought that these residues could not participate in hydrophobic contacts with the inhibitor seen in the crystal structure of the phenylC3SH complex, reflecting the difference

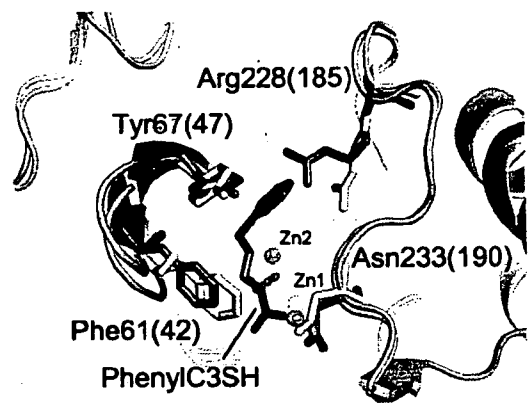

Figure 4. Conformational changes in loops 1 and 2 upon phenylC3SH binding to the VIM-2 enzyme. Superposition of native VIM-2 (green) (PDB code 1KO3) and the phenylC3SH complex (yellow). Molecule A of the phenylC3SH complex is depicted and the amino acid residues of VIM-2 are designated with a BBL number and an amino acid sequence number; the latter is in parentheses. Phe61(42), Tyr67(47), Arg228(185), and Asn233(190) residues are presented as balls and sticks. Zn(II) ions are shown as orange spheres. PhenylC3SH is presented as a stick (carbon, oxygen, and sulfur atoms are shown in magenta, red, and light-green, respectively). The figure was prepared with PyMol software (http://pymol.sourceforgen.net/).

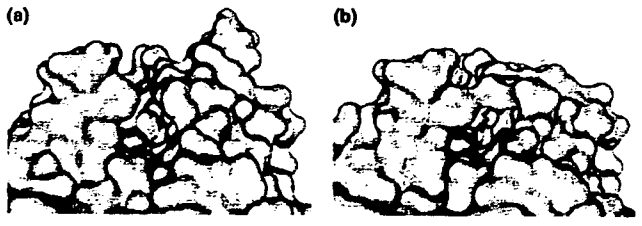

Figure 5. Molecular surface representations of native VIM-2 (a) and the phenylC3SH complex (b). In the phenylC3SH complex, molecule A is depicted as a molecular surface. The amino acid residues of VIM-2 are designated with a BBL number and an amino acid sequence number; the latter is in parentheses. Zn(II) ion (Zn2) is shown as an orange sphere. PhenylC3SH is presented as a stick (carbon, oxygen, and sulfur atoms are shown in magenta, red, and light-green, respectively). The figure was prepared with PyMol software (http://pymol.sourceforgen.net/).

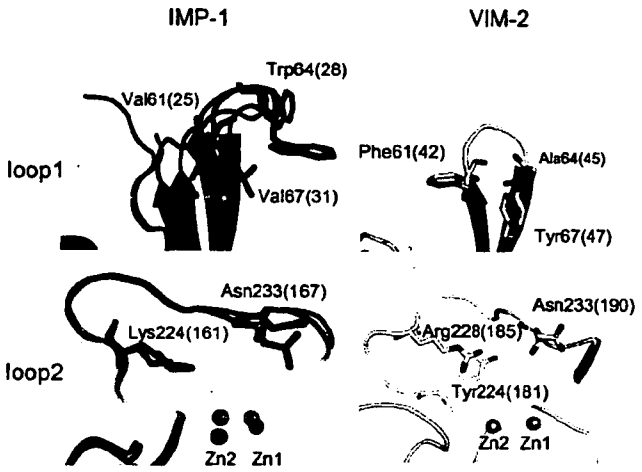

Figure 6. Comparison of loops 1 and 2 between IMP-1 and VIM-2 enzymes. The amino acid residues of the IMP-1 and VIM-2 enzymes are designated with a BBL number and an amino acid sequence number; the latter is in parentheses. In the IMP-1 enzyme (left), the structures of IMP-1 metallo-β-lactamase from *P. aeruginosa* (PDB code 1DDK) (red) and its complex with a mercaptocarboxylate inhibitor (PDB code 1DD6, molecule A is depicted) (blue) were used for comparison,[22] but the inhibitor 2-[5-(1-tetrazoylmethyl)thien-3-yl]-*N*-[2-(mercaptomethyl)-4-(phenylbutyrylglycine)] was omitted for clarity. Val61(25), Trp64(28), and Val67(31) residues on loop1 and Lys224(161) and Asn233(167) residues on loop2 are presented as sticks (carbon, gray; nitrogen, blue; oxygen, red). Zn(II) ions are shown as orange spheres. In the VIM-2−phenylC3SH complex (right), molecule A is depicted and phenylC3SH was omitted for clarity. Phe61(42), Ala64(45), and Tyr67(47) residues on loop1 and Tyr224(181), Arg228(185), and Asn233(190) residues of the VIM-2 enzyme are presented as sticks (carbon, gray; nitrogen, blue; oxygen, red). Zn(II) ions are shown as orange spheres. The figure was prepared with the PyMol software program (http://pymol.sourceforgen.net/).

in inhibitory activity of phenylC3SH between the VIM-2 and IMP-1 enzymes.

Lys224(161) in the IMP-1 enzyme is located on loop2, which is ~5 Å away from the Zn(II) center. In the mercaptocarboxylate inhibitor complex, the carboxyl group of inhibitor interacts with the side chain NZ of Lys224(161) with a distance of 2.8 Å, and this result shows the importance of Lys224(161) in inhibitor binding. Moreover, Lys224(161) is assumed to interact with the carboxylate of the β-lactam antibiotics.[22,31] However, in the case of the VIM-2 enzyme, Lys224(161) is replaced with Tyr224(181). On the basis of the crystal structure of the phenylC3SH complex, Arg228(185) near Tyr224(181) on loop2 might aid in carrying out the role of Lys224(161) in IMP-1.

It is noteworthy that the movement and rotation of Asn233(190) occur upon inhibitor binding to the VIM-2 enzyme. In the crystal structure of the IMP-1−mercaptocarboxylate inhibitor complex,[22] a similar behavior was observed, where the carbonyl oxygen of the inhibitor is oriented for interaction with the side chain ND2 of Asn233(167) (4.1 Å) in an oxyanion hole.[31] From the above results it can be concluded that the role of Asn233(190) in the VIM-2 structure is to stabilize either a substrate or an inhibitor.

Conclusion

We determined the three-dimensional structure of a VIM-2 enzyme complexed with a mercaptocarboxylate inhibitor, phenylC3SH, which is the first VIM family member to be characterized as being complexed with an inhibitor. From the results of the crystal structure, the precise inhibition mode of the VIM-2 enzyme with phenylC3SH was ascertained: in particular, Phe61(42) and Tyr67(47), located in loop1 and Arg228(185) and Asn233(190) in loop2 play an important role in the binding and recognition of the inhibitor to the VIM-2 enzyme and in the stabilization of the VIM-2 structure. Moreover, Phe61 and Tyr67 residues are conserved in the other members of subclass B1 MBLs: VIM-1,[38] BlaB,[39] and IND-1.[40] Therefore, in these MBLs, two residues seem to play the same role, as can been seen in this study.

These findings would aid in the design of inhibitors that target not only VIM-2 but also other MBLs.

Experimental Section

Expression and Purification. The VIM-2 metallo-β-lactamse was expressed by *Escherichia coli* NCB326-1B2 harboring pVM4k/VIM-2 and purified as previously described.[30]

Synthesis of Inhibitor. *rac*-2-(ω-Phenylpropyl-3-mercaptopropionic acid, phenylC3SH, was synthesized by the method described by Park et al.[41]

Crystallization of the VIM-2 Enzyme Complexed with PhenylC3SH. Prior to the X-ray diffraction experiments, a buffer solution of the VIM-2 enzyme was converted from Tris-HCl (50 mM, pH 7.4, 0.5 M NaCl) to HEPES−NaOH (20 mM, pH 7.5) and the VIM-2 protein was then concentrated to about 5 mg/mL (160 μM) on a Centricon. Drops of the VIM-2 protein with phenylC3SH were prepared by mixing 2 μL of a concentrated protein solution, 2 μL of a reservoir solution (30% PEG MME5000, 0.1 M MES−NaOH, and 0.2 M ammonium sulfate (pH 6.5)), and 1 μL of a methanolic phenylC3SH solution (10 mM). The crystals were grown for two months as plates (0.4 mm × 0.4 mm × 0.2 mm) at 20 C°.

Data Collection and Processing. Cocrystals of the VIM-2 enzyme with phenylC3SH were mounted in nylon loops directly from the mother liquor and flash-cooled in liquid nitrogen stream (100 K). All diffraction data were collected on beamline BL40B2 using an ADSC Quantum-4R detector at 100 K and beamline BL41XU using a marCCD 165 detector at 100 K at SPring-8 (Harima, Japan). A full MAD data collection around the zinc edge was performed with a single frozen crystal at SPring-8 BL40B2. Diffraction data were collected by the oscillation method at three carefully selected wavelengths: λ_1 = 1.2826 Å (edge, f'minimum), λ_2 = 1.2817 Å (peak, f' maximum), and λ_3 = 1.2906 Å (remote high-energy wavelength). After completion of the MAD data collection at a resolution of 2.55 Å, a data set of 360 frames at λ = 1.0000 Å was collected at a resolution of 2.3 Å with 0.5° oscillation steps at SPring-8 BL41XU. The data were integrated and scaled with HKL2000.[42]

Phasing, Structure Determination, Model Building, and Refinement. Phase determination for the VIM-2 enzyme complexed with phenylC3SH was performed using the SOLVE program[43] and density modification, and model building was performed with the RESOLVE program.[44] This led to an interpretable density map and

an initial map. The O[45] and Coot[46] programs were further used in modeling and remodeling. The refinement was carried out using REFMAC5,[47] a component of the CCP4 suite,[48] and CNS[49] programs without a noncrystallographic symmetry (NCS). PhenylC3SH was built and minimized in MOE (CCG Inc., Canada), and the topology and parameter files of phenylC3SH were utilized in PRPDRG (http://davapc1.bioch.dundee.ac.uk/programs/prodrg/).[50] The quality of the model was inspected by the program PROCHECK.[51] Data collection and refinement statistics can be found in Table 1. The atomic coordinates and structure factors (PDB code 2YZ3) have been deposited at the Protein Data Bank, Research Collaboratory for Structural Bioinformatics, Rutgers University, New Brunswick, NJ (http://www.rcsb.org/).

In the case of the IMP-1 enzyme, however, we were unable to examine the IMP-1 enzyme complexed with phenylC3SH by X-ray crystallography because of the poor quality of the crystals obtained.

Acknowledgment. Work related to the preparation, purification, and X-ray crystallographical studies of the enzymes was supported by a Grant from the Ministry of Health, Labor, and Welfare of Japan (H18-Shinkou-11). The synthetic study was supported by a Grant-in-Aid for Scientific Research (B) (Grant No. 18390038) and Grant-in-Aid for Young Scientists (B) (Grant No. 18790028) from the Japan Society for the Promotion of Science.

References

(1) Cricco, J. A.; Vila, A. J. Class B β-lactamases: the importance of being metallic. *Curr. Pharm. Des.* **1999**, *5*, 915–927.
(2) Page, M. I. The reactivity of β-lactams, the mechanism of catalysis and the inhibition of β-lactamases. *Curr. Pharm. Des.* **1999**, *5*, 895–913.
(3) Ambler, R. P. The structure of β-lactamases. *Phil. Trans. R. Soc. London, Ser. B* **1980**, *289*, 321–331.
(4) Babic, M.; Hujer, A. M.; Bonomo, R. A. What's new in antibiotic resistance? Focus on beta-lactamases. *Drug Resist. Updates* **2006**, *9*, 142–156.
(5) Fisher, J. F.; Meroueh, S. O.; Mobashery, S. Bacterial resistance to β-lactam antibiotics: compelling opportunism, compelling opportunity. *Chem. Rev.* **2005**, *105*, 395–424.
(6) Galleni, M.; Lamotte-Brasseur, J.; Rossolini, G. M.; Spencer, J.; Dideberg, O.; Frère, J.-M. The metallo-β-lactamase working group Standard numbering scheme for class B β-lactamases. *Antimicrob. Agents Chemother.* **2001**, *45*, 660–663.
(7) Heinz, U.; Adolph, H.-W. Metallo-β-lactamases: two binding sites for one catalytic metal ion. *Cell. Mol. Life Sci.* **2004**, *61*, 2827–2839.
(8) Hussain, M.; Carlino, A.; Madonna, M. J.; Lampen, J. O. Cloning and sequencing of the metallothioprotein β-lactamase II gene of *Bacillus cereus* 569/H in *Escherichia coli*. *J. Bacteriol.* **1985**, *164*, 223–229.
(9) Walsh, T. R.; Toleman, M. A.; Poirel, L.; Nordmann, P. Metallo-β-lactamases: the quiet before the storm. *Clin. Microbiol. Rev.* **2005**, *18*, 306–325.
(10) Rasmussen, B. A.; Gluzman, Y.; Tally, F. P. Cloning and sequencing of the class B β-lactamase gene (*ccrA*) from *Bacteroides fragilis* TAL3636. *Antimicrob. Agents Chemother.* **1990**, *34*, 1590–1592.
(11) Massidda, O.; Rossolini, G. M.; Satta, G. The *Aeromonas hydrophila cphA* gene: molecular heterogeneity among class B metallo-β-lactamases. *J. Bacteriol.* **1991**, *173*, 4611–4617.
(12) Walsh, T. R.; Gamblin, S.; Emery, D. C.; MacGowan, A. P.; Bennett, P. M. Enzyme kinetics and biochemical analysis of ImiS, the metallo-β-lactamase from *Aeromonas sobria* 163a. *J. Antimicrob. Chemother.* **1996**, *37*, 423–431.
(13) Walsh, T. R.; Hall, L.; Assinder, S. J.; Nichols, W. W.; Cartwright, S. J.; MacGowan, A. P.; Bennett, P. M. Sequence analysis of the L1 metallo-β-lactamase from *Xanthomonas maltophilia*. *Biochim. Biophys. Acta* **1994**, *1218*, 199–201.
(14) Rossolini, G. M.; Condemi, M. A.; Pantanella, F.; Docquier, J.-D.; Amicosante, G.; Thaller, M. C. Metallo-β-lactamase producers in environmental microbiota: new molecular class B enzyme in *Janthinobacterium lividum*. *Antimicrob. Agents Chemother.* **2001**, *45*, 837–844.
(15) Poirel, L.; Naas, T.; Nicolas, D.; Collet, L.; Bellais, S.; Cavallo, J.-D.; Nordmann, P. Characterization of VIM-2, a carbapenem-hydrolyzing metallo-β-lactamase and its plasmid- and integron-borne gene from a *Pseudomonas aeruginosa* clinical isolate in France. *Antimicrob. Agents Chemother.* **2000**, *44*, 891–897.
(16) Moali, C.; Anne, C.; Lamotte-Brasseur, J.; Groslambert, S.; Devreese, B.; Van Beeumen, J.; Galleni, M.; Frère, J.-M. Analysis of the importance of the metallo-β-lactamase active site loop in substrate binding and catalysis. *Chem. Biol.* **2003**, *10*, 319–329.
(17) Huntley, J. J. A.; Scrofani, S. D. B.; Osborne, M. J.; Wright, P. E.; Dyson, H. J. Dynamics of the metallo-β-lactamase from *Bacteroides fragilis* in the presence and absence of a tight-binding inhibitor. *Biochemistry* **2000**, *39*, 13356–13364.
(18) Huntley, J. J.; Fast, W.; Benkovic, S. J.; Wright, P. E.; Dyson, H. J. Role of a solvent-exposed tryptophan in the recognition and binding of antibiotic substrates for a metallo-β-lactamase. *Protein Sci.* **2003**, *12*, 1368–1375.
(19) Scrofani, S. D. B.; Chung, J.; Huntley, J. J. A.; Benkovic, S. J.; Wright, P. E.; Dyson, H. J. NMR characterization of the metallo-β-lactamase from *Bacteroides fragilis* and its interaction with a tight-binding inhibitor: role of an active-site loop. *Biochemistry* **1999**, *38*, 14507–14514.
(20) Docquier, J.-D.; Lamotte-Brasseur, J.; Galleni, M.; Amicosante, G.; Frère, J.-M.; Rossolini, G. M. On functional and structural heterogeneity of VIM-type metallo-β-lactamases. *J. Antimicrob. Chemother.* **2003**, *51*, 257–266.
(21) Salsbury, F. R., Jr.; Crowley, M. F.; Brooks, C. L., III. Modeling of the metallo-β-lactamase from *B. fragilis*: structural and dynamic effects of inhibitor binding. *Proteins. Struct., Funct., Genet.* **2001**, *44*, 448–459.
(22) Concha, N. O.; Janson, C. A.; Rowling, P.; Pearson, S.; Cheever, C. A.; Clarke, B. P.; Lewis, C.; Galleni, M.; Frère, J.-M.; Payne, D. J.; Bateson, J. H.; Abdel-Meguid, S. S. Crystal structure of the IMP-1 metallo β-lactamase from *Pseudomonas aeruginosa* and its complex with a mercaptocarboxylate inhibitor: binding determinants of a potent, broad-spectrum inhibitor. *Biochemistry* **2000**, *39*, 4288–4298.
(23) Fitzgerald, P. M. D.; Wu, J. K.; Toney, J. H. Unanticipated inhibition of the metallo-β-lactamase from *Bacteroides fragilis* by 4-morpholineethanesulfonic acid (MES): a crystallographic study at 1.85-Å resolution. *Biochemistry* **1998**, *37*, 6791–6800.
(24) Toney, J. H.; Fitzgerald, P. M. D.; Grover-Sharma, N.; Olson, S. H.; May, W. J.; Sundelof, J. G.; Vanderwall, D. E.; Cleary, K. A.; Grant, S. K.; Wu, J. K.; Kozarich, J. W.; Pompliano, D. L.; Hammond, G. G. Antibiotic sensitization using biphenyl tetrazoles as potent inhibitors of *Bacteroides fragilis* metallo-β-lactamase. *Chem. Biol.* **1998**, *5*, 185–196.
(25) Toney, J. H.; Hammond, G. G.; Fitzgerald, P. M. D.; Sharma, N.; Balkovec, J. M.; Rouen, G. P.; Olson, S. H.; Hammond, M. L.; Greenlee, M. L.; Gao, Y.-D. Succinic acids as potent inhibitors of plasmid-borne IMP-1 metallo-β-lactamase. *J. Biol. Chem.* **2001**, *276*, 31913–31918.
(26) Kurosaki, H.; Yamaguchi, Y.; Higashi, T.; Soga, K.; Matsueda, S.; Yumoto, H.; Misumi, S.; Yamagata, Y.; Arakawa, Y.; Goto, M. Irreversible inhibition of metallo-β-lactamase (IMP-1) by 3-(3-mercaptopropionylsulfanyl)propionic acid pentafluorophenyl ester. *Angew. Chem., Int. Ed.* **2005**, *44*, 3861–3864.
(27) Kurosaki, H.; Yamaguchi, Y.; Yasuzawa, H.; Jin, W.; Yamagata, Y.; Arakawa, Y. Probing, inhibition, and crystallographic characterization of metallo-β-lactamase (IMP-1) with fluorescent agents containing dansyl and thiol groups. *ChemMedChem* **2006**, *1*, 969–972.
(28) García-Sáez, I.; Hopkins, J.; Papamicael, C.; Franceschini, N.; Amicosante, G.; Rossolini, G. M.; Galleni, M.; Frère, J.-M.; Dideberg, O. The 1.5-Å structure of *Chryseobacterium meningosepticum* zinc β-lactamase in complex with the inhibitor, D-captopril. *J. Biol. Chem.* **2003**, *278*, 23868–23873.
(29) García-Sáez, I.; Mercuri, P. S.; Papamicael, C.; Kahn, R.; Frère, J.-M.; Galleni, M.; Rossolini, G. M.; Dideberg, O. Three-dimensional structure of FEZ-1, a monomeric subclass B3 metallo-β-lactamase from *Fluoribacter gormanii*, in native form and in complex with D-captopril. *J. Mol. Biol.* **2003**, *325*, 651–660.
(30) Jin, W.; Arakawa, Y.; Yasuzawa, H.; Taki, T.; Hashiguchi, R.; Mitsutani, K.; Shoga, A.; Yamaguchi, Y.; Kurosaki, H.; Shibata, N.; Ohta, M.; Goto, M. Comparative study of the inhibition of metallo-β-lactamases (IMP-1 and VIM-2) by thiol compounds that contain a hydrophobic group. *Biol. Pharm. Bull.* **2004**, *27*, 851–856.
(31) Concha, N. O.; Rasmussen, B. A.; Bush, K.; Herzberg, O. Crystal structure of the wide-spectrum binuclear zinc β-lactamase from *Bacteroides fragilis*. *Structure* **1996**, *4*, 823–836.
(32) Carfi, A.; Pares, S.; Duée, E.; Galleni, M.; Duez, C.; Frère, J.-M.; Dideberg, O. The 3-D structure of a zinc metallo-β-lactamase from *Bacillus cereus* reveals a new type of protein fold. *EMBO J.* **1995**, *14*, 4914–4921.
(33) De La Sierra-Gallay, I. L.; Pellegrini, O.; Condon, C. Structural basis for substrate binding, cleavage and allostery in the tRNA maturase RNase Z. *Nature* **2005**, *433*, 657–661.
(34) Mandel, C. R.; Kaneko, S.; Zhang, H.; Gebauer, D.; Vethantham, V.; Manley, J. L.; Tong, L. Polyadenylation factor CPSF-73 is the pre-mRNA 3′-end-processing endonuclease. *Nature* **2006**, *444*, 953–956.

(35) Wang, Z.; Benkovic, S. J. Purification, characterization, and kinetic studies of a soluble *Bacteroides fragilis* metallo-β-lactamase that provides multiple antibiotic resistance. *J. Biol. Chem.* **1998**, *273*, 22402–22408.

(36) Wang, Z.; Fast, W.; Valentine, A. M.; Benkovic, S. J. Metallo-β-lactamase: structure and mechanism. *Curr. Opin. Chem. Biol.* **1999**, *3*, 614–622.

(37) Wang, Z.; Fast, W.; Benkovic, S. J. Direct observation of an enzyme-bound intermediate in the catalytic cycle of the metallo-β-lactamase from *Bacteroides fragilis*. *J. Am. Chem. Soc.* **1998**, *120*, 10778–10789.

(38) Lauretti, L.; Riccio, M. L.; Mazzariol, A.; Cornaglia, G.; Amicosante, G.; Fontana, R.; Rossolini, G. M. Cloning and characterization of bla_{VIM}, a new integron-borne metallo-β-lactamase gene from a *Pseudomonas aeruginosa* clinical isolate. *Antimicrob. Agents Chemother.* **1999**, *43*, 1584–1590.

(39) Rossolini, G. M.; Franceschini, N.; Riccio, M. L.; Mercuri, P. S.; Perilli, M.; Galleni, M.; Frère, J.-M.; Amicosante, G. Characterization and sequence of the *Chryseobacterium* (*Flavobacterium*) *meningosepticum* carbapenemase: a new molecular class B β-lactamase showing a broad substrate profile. *Biochem. J.* **1998**, *332*, 145–152.

(40) Bellais, S.; Léotard, S.; Poirel, L.; Naas, T.; Nordmann, P. Molecular characterization of a carbapenem-hydrolyzing β-lactamase from *Chryseobacterium* (*Flavobacterium*) indologenes. *FEMS Microbiol. Lett.* **1999**, *171*, 127–132.

(41) Park, J. D.; Kim, D. H. Cysteine derivatives as inhibitors for carboxypeptidase A: synthesis and structure−activity relationships. *J. Med. Chem.* **2002**, *45*, 911–918.

(42) Otwinowski, Z.; Minor, W. Processing of X-ray diffraction data collected in oscillation mode. *Methods Enzymol.* **1997**, *276*, 307–326.

(43) Terwilliger, T. C.; Berendzen, J. Automated MAD and MIR structure solution. *Acta Crystallogr., Sect. D: Biol. Crystallogr.* **1999**, *55*, 849–861.

(44) Terwilliger, T. C. Maximum-likelihood density modification. *Acta Crystallogr., Sect. D: Biol. Crystallogr.* **2000**, *56*, 965–972.

(45) Jones, T. A.; Zou, J.-Y.; Cowan, S. W.; Kjeldgaard, M. Improved methods for building protein models in electron density maps and the location of errors in these models. *Acta Crystallogr., Sect. A: Found. Crystallogr.* **1991**, *47*, 110–119.

(46) Emsley, P.; Cowtan, K. Coot: model-building tools for molecular graphics. *Acta Crystallogr., Sect. D: Biol. Crystallogr.* **2004**, *60*, 2126–2132.

(47) Murshudov, G. N.; Vagin, A. A.; Dodson, E. J. Refinement of macromolecular structures by the maximum-likelihood method. *Acta Crystallogr., Sect. D: Biol. Crystallogr.* **1997**, *53*, 240–255.

(48) Collaborative Computational Project Number 4. The CCP4 suite: programs for protein crystallography. *Acta Crystallogr., Sect. D: Biol. Crystallogr.* **1994**, *50*, 760–763.

(49) Brünger, A. T.; Adams, P. D.; Clore, G. M.; DeLano, W. L.; Gros, P.; Grosse-Kunstleve, R. W.; Jiang, J.-S.; Kuszewski, J.; Nilges, M.; Pannu, N. S.; Read, R. J.; Rice, L. M.; Simonson, T.; Warren, G. L. Crystallography & NMR system: a new software suite for macromolecular structure determination. *Acta Crystallogr., Sect. D: Biol. Crystallogr.* **1998**, *54*, 905–921.

(50) Schüttelkopf, A. W.; Van Aaltena, D. M. PRODRG: a tool for high-throughput crystallography of protein−ligand complexes. *Acta Crystallogr., Sect. D: Biol. Crystallogr.* **2004**, *6*, 1355–1363.

(51) Laskowski, R. A.; MacArthur, M. W.; Moss, D. S.; Thornton, J. M. PROCHECK: a program to check the stereochemical quality of protein structures. *J. Appl. Crystallogr.* **1993**, *26*, 283–291.

JM701031N

JOURNAL OF CLINICAL MICROBIOLOGY, Sept. 2007, p. 2813–2818 Vol. 45, No. 9
0095-1137/07/$08.00+0 doi:10.1128/JCM.00457-07

Molecular Characterization of Vancomycin-Resistant *Enterococcus faecium* Isolates from Mainland China▽

Bo Zheng,[1,3] Haruyoshi Tomita,[1]* Yong Hong Xiao,[3] Shan Wang,[3] Yun Li,[3] and Yasuyoshi Ike[1,2]

Department of Bacteriology and Bacterial Infection Control[1] and Laboratory of Bacterial Drug Resistance,[2] Gunma University Graduate School of Medicine, Maebashi, Gunma 371-8511, Japan, and Institute of Clinical Pharmacology, Peking University First Hospital, Beijing 100034, China[3]

Received 28 February 2007/Returned for modification 20 April 2007/Accepted 11 June 2007

Little is known about vancomycin-resistant enterococci in China. Thirteen pulsed-field gel electrophoresis-confirmed heterogeneous VanA-type vancomycin-resistant *Enterococcus faecium* (VRE) isolates were obtained from five Chinese hospitals from 2001 to 2005. The isolates were typed by multilocus sequence typing into nine different sequence types (STs), including five new STs (ST18, ST25, ST78, ST203, ST320, ST321, ST322, ST323, and ST335). Vancomycin resistance in each isolate was encoded on conjugative plasmids; two of the plasmids, pZB18 (67 kbp) and pZB22 (200 kbp), were highly conjugative and were able to transfer at high frequencies of around 10^{-4} and 10^{-7} per donor cell in broth mating, respectively. None of the plasmids identified in these isolates carried *traA*, which is usually conserved in the pMG1-like highly conjugative plasmid for *E. faecium*, implying that pZB18 and pZB22 were novel types of a highly conjugative plasmid in enterococci. Thirteen Tn*1546*-like elements encoding VanA-type VRE on the conjugative plasmids were classified into six types (types I to VI), and most of them contained both IS*1216V* and IS*1542* insertions. The isolates carrying the type II element were predominant. The six type elements were different from that of a VanA-type *Enterococcus faecalis* strain isolated from Chinese chicken meat. The results suggested that the disseminations of VRE in these areas were by Tn*1546*-like elements being acquired by the conjugative plasmids and transferred among *E. faecium* strains.

The isolation of vancomycin-resistant enterococci (VRE) was first reported in 1988 in the United Kingdom and France (17, 29) and then in hospitals in the United States (20). VRE are now encountered in many countries, especially in Europe and the United States (2). There are several reports describing the isolation of VRE in East Asian regions and countries, including Japan, Korea, and Taiwan, and isolation frequencies of VRE from patients and food animals have been increasing both in Korea and in Taiwan (15, 34). Since the first Japanese report of a VanA-type VRE (*Enterococcus faecium*) clinical isolate in 1996, the frequencies of VRE isolation from patients have also increased (7, 18). However, little information is available on the prevalence of VRE and their molecular makeup from mainland China, although glycopeptide antimicrobials have been used there for decades.

VanA-type resistance, characterized by high-level inducible vancomycin resistance (MICs of 64 to >1,024 μg/ml) and teicoplanin resistance (MICs of 16 to >512 μg/ml), is most frequently encountered (19). The genes encoding VanA-type vancomycin resistance are located on mobile Tn*1546*-like elements; therefore, the horizontal transfer of resistance genes among enterococci has a more significant impact on the dissemination of VRE than does the clonal spread of resistant enterococci (14). Epidemiological studies of VanA-type enterococci indicate that there are geographic differences (22). Considerable diversity has been identified in the Tn*1546*-related elements. This variation, in the form of point mutations, insertion sequence (IS) elements, and deletions, has been exploited in several epidemiological studies (33, 31).

Vancomycin has been used in patient care in mainland China for 40 years, and its usage is increasing. Our group has previously described vancomycin-dependent VanA-type VRE strains isolated in Japan from retail chicken meat imported from China (25). Clinical isolates of VanA-type VRE (*E. faecium*) are rarely obtainable from China. Over the past five years, we have obtained a total of 13 clinical strains of VanA-type VRE (*E. faecium*) from China. The current report is the first to describe molecular characterization of VanA-type VRE from mainland China.

MATERIALS AND METHODS

Bacterial strains and culture media. Thirteen clinical isolates of vancomycin-resistant *E. faecium* recovered from blood cultures and urine and sputum samples from patients in China were used in this study (Table.1). VanA-type vancomycin-resistant *Enterococcus faecalis* strain KC122.1, isolated in Japan from chicken meat imported from China in 2001, was used for the comparative analysis of Tn*1546*-like elements (25). *E. faecium* strains BM4105RF and BM4105SS were used as recipient strains for transfer experiments (13). Enterococci were grown in Todd-Hewitt broth (THB).

Antimicrobial susceptibility testing. Glycopeptide resistance levels were determined by the agar dilution method. An overnight pure culture of each strain grown in Mueller-Hinton broth (Nissui, Tokyo, Japan) was diluted 100-fold with fresh broth. An inoculum of approximately 5×10^5 cells was plated on a series of Mueller-Hinton agar plates (Eiken, Tokyo, Japan) containing a range of concentrations of the test drug. The plates were incubated at 37°C, and the susceptibility results were finalized at 24 h of incubation. Susceptibility testing and interpretation of results were in compliance with standards recommended by

* Corresponding author. Mailing address: Bacteriology and Bacterial Infection Control, Gunma University Graduate School of Medicine, 3-39-22 Showa-machi, Maebashi, Gunma 371-8511, Japan. Phone: 81-27-220-7992. Fax: 81-27-220-7996. E-mail: tomitaha@med.gunma-u.ac.jp.

▽ Published ahead of print on 18 July 2007.

TABLE 1. Chinese VanA-type vancomycin-resistant *E. faecium* clinical isolates[a]

Strain	Hospital (city)	Date of isolation (yr/mo/day)	Source	Diagnosis/underlying disease[b]	Antibiotic(s) used	MLST result[c]							
						Sequence type (nearest)	Clonal complex	Allelic profile					
								atpA	*ddl*	*gdh*	*purK*	*gyd*	*pstS*	*adkC*
1125	E (Dalian)	2001/12/9	Sputum	Cachexia/gastric cancer	CEPs, CLI	ST78	CC78	15	1	1	1	1	1	1
C264	A (Beijing)	2003/8/21	Bile	Cholangitis/hepatocirrhosis	VAN, CEPs	ST320* (ST80)	CC117	9	1	1	1	12	29	1
ZB11	A (Beijing)	2004/1/15	Urine	Pyelitis/gastric cancer	VAN	ST335* (ST172)	CC5	45*	13	34*	15	19	29	18*
ZB14	B (Beijing)	2004/2/13	Urine	Pyelitis/leukemia	CEPs	ST321* (ST31)	CC280	7	3	1	1	1	1	3
ZB15	B (Beijing)	2004/2/27	Urine	Pyelitis/kidney dysfunction	TEC	ST78	CC78	15	1	1	1	1	1	1
ZB16	B (Beijing)	2004/4/4	Urine	Pyelitis/hepatocirrhosis	CEPs	ST18	CC18	7	1	1	1	5	1	1
ZB18	B (Beijing)	2004/4/9	Blood	Sepsis/leukemia	VAN, CEPs	ST25	CC25	9	3	1	6	1	1	1
ZB19	C (Beijing)	2005/10/18	Sputum	Pneumonia/pulmonary dysfunction	VAN, CEPs	ST322* (ST262)	CC18	7	1	6	1	5	7	1
ZB20	C (Beijing)	2005/10/20	Urine	Pyelitis/rectal cancer	VAN, CEPs	ST203	CC78	15	1	1	1	1	20	1
ZB21	D (Tianjin)	2005/10/12	Blood	Sepsis/hepatocellular cancer	VAN, MEM	ST78	CC78	15	1	1	1	1	1	1
ZB22	B (Beijing)	2005/10/28	Sputum	Pneumonia/COPD	VAN, MEM	ST323* (ST17)	CC17	5	1	1	1	1	1	1
ZB23	C (Beijing)	2005/11/7	Sputum	Pneumonia/bronchiectasis	CEPs	ST203	CC78	15	1	1	1	1	20	1
ZB24	C (Beijing)	2005/11/8	Urine	Pyelitis/COPD	CEPs	ST203	CC78	15	1	1	1	1	20	1

[a] Drug abbreviations: CEPs, broad-spectrum cephalosporins; CLI, clindamycin; VAN, vancomycin; TEC, teicoplanin; MEM, meropenem; AMP, ampicillin; GEN, gentamicin; STR, streptomycin; TET, tetracycline; ERY, erythromycin; CHL, chloramphenicol; RIF, rifampin; LVX, levofloxacin; LZD, linezolid.
[b] COPD, chronic obstructive pulmonary disease.
[c] *, new ST/allele in this study.
[d] The *esp* gene was detected by PCR amplification, as described in the text. P, positive; N, negative.
[e] Tn*1546*-like elements were typed by DNA sequence structure, as shown in Fig. 4.
[f] The wild-type strain and *E. faecium* BM4105RF were used as donor and recipient, respectively (13).
[g] Plasmids were identified in our previous report (35).

Clinical Laboratory Standards Institute (formerly NCCLS). *E. faecium* ATCC 9790 was used as a control strain.

Plasmid DNA methods. Recombinant DNA methodology, analyses of plasmid DNA with restriction enzymes, and agarose gel electrophoresis were carried out by standard methods (21). PCR was performed with a Perkin-Elmer Cetus apparatus. Specific primers for DNA sequencing of the Tn*1546*-like element and insertion sequences were designed as previously reported and purchased from Invitrogen (11, 31, 22, 34). Sequence analysis was performed with a dye terminator cycle sequencing kit (Applied Biosystems) and a model 310 gene analyzer (ABI PRISM).

Conjugation experiments. Broth matings were performed as previously described with a donor/recipient ratio of 1:10 (5, 12). Overnight cultures of 0.05 ml of the donor and 0.45 ml of the recipient were added to 4.5 ml of fresh THB, and the mixtures were incubated at 37°C with gentle agitation for the appropriate times and then vortexed. Portions of the mixed cultures were then plated on solid media with appropriate selective antibiotics. Colonies were counted after 48 h of incubation at 37°C. Filter matings were performed as previously described with a donor/recipient ratio of 1:10 (6). Overnight cultures were prepared, 0.05 ml of the donor and 0.5 ml of the recipient were added to 4.5 ml of fresh THB, and the cells were then trapped on a membrane filter (Millipore, Bedford, MA). The cells on the filters were incubated at 37°C overnight and were then suspended in 1 ml of THB. Appropriate dilutions of the mixture were transferred to plates of solid medium containing selective antibiotics. Throughout the mating experiments, the antibiotic concentration used for the selection of vancomycin-resistant transconjugants was 6 μg/ml. The antibiotic concentrations used for the selection of rifampin- and fusidic acid-resistant recipient strains or streptomycin- and spectinomycin-resistant recipient strains were 25 and 25 μg/ml or 250 and 250 μg/ml, respectively.

PFGE. Pulsed-field gel electrophoresis (PFGE) was then carried out in a 1% agarose gel with 0.5% Tris-borate-EDTA buffer, and the following settings were applied: 1 to 23 s, 6 V/cm, and 22 h (with the CHEF Mapper system [Bio-Rad]) (18).

DNA-DNA hybridization. Southern hybridization was performed with the digoxigenin-based nonradioisotope system of Boehringer GmbH (Mannheim, Germany), and all procedures were based on the manufacturer's manual (21).

MLST analysis. Multilocus sequence typing (MLST) analysis of *E. faecium* isolates was performed as previously reported (10, 32). The alleles and sequence types (STs) were analyzed and determined through the MLST database (http://efaecium.mlst.net/). The new alleles and new STs identified in this study have been deposited in the database.

Detection of the *esp* gene. To detect the *esp* gene of the *E. faecium* isolates, PCR amplification was performed as previously described with specific primers (16).

Detection of the *traA* gene of a pMG1-like plasmid. To detect the *traA* gene in the conjugative plasmids, PCR amplification was performed with specific primers (traA-F, TGAGAAAGAAATCGCTGATG; traA-R, TGAAGGCGTTCTTCT TTCAG), as previously described (24, 28).

RESULTS AND DISCUSSION

Isolation and characterization of VanA-type vancomycin-resistant *E. faecium*. The characteristics of the 13 isolates of vancomycin-resistant *E. faecium* are listed in Table 1. Each VRE strain was isolated from an individual patient in the hospital. In all cases, glycopeptide antibiotics and/or broad-spectrum cephalosporins were administrated to the patient before the isolation of VRE. All isolates were multidrug resistant, with MICs of 256 to 512 μg/ml and 16 to 512 μg/ml for vancomycin and teicoplanin, respectively. All 13 *E. faecium* isolates were resistant to erythromycin, and 11 isolates (85%) also showed high-level resistance to ampicillin and gentamicin. All isolates were sensitive to linezolid.

The PFGE profiles of SmaI-digested chromosomal DNA demonstrated that strain ZB23 was closely related to strain ZB24, differing by only one band; the other 11 isolates were largely heterogeneous in nature (Fig. 1), indicating that these isolates were unrelated and suggesting that vancomycin resistance was able to emerge in different *E. faecium* strains.

MLST analysis. All isolates were analyzed by the MLST scheme for *E. faecium* described previously (10, 32; http://www.mlst.net). Allelic profiles of these *E. faecium* isolates were obtained by sequencing of internal fragments of seven housekeeping genes—*atpA*, *ddl*, *gdh*, *purK*, *gyd*, *pstS*, and *adkC*—and STs were determined (Table 1). In strain ZB18, three of seven alleles, *atpA*, *adh*, and *pdkC*, belonged to the new alleles, and the closest homologue alleles found were between *atpA* and *atpA15* (81% identity), *adh* and *gdh19* (99% identity), and *pdkC* and *adkC8* (81% identity). Based on the allelic profiles of the 13 isolates, three belonged to ST78 and three to ST203,

TABLE 1—*Continued*

esp status[d]	Tn*1546*-like element		Transfer frequency of vancomycin resistance[f] (per donor cell)		MIC (μg/ml)										
	Type[e]	Location	Broth mating (4 h)	Filter mating (16 h)	VAN	TEC	AMP	GEN	STR	TET	ERY	CHL	RIF	LVX	LZD
N	VI	Plasmid (pI125V^S)	$<10^{-7}$	1.6×10^{-4}	512	16	128	>1,024	2048	0.5	512	8	4	16	2
N	V	Plasmid (pC264V^S)	$<10^{-7}$	2.3×10^{-7}	256	32	128	>1,024	64	0.5	512	32	4	32	2
N	II	Plasmid	$<10^{-7}$	3.0×10^{-5}	512	256	0.25	>1,024	32	0.5	512	16	512	1	2
N	II	Plasmid	$<10^{-7}$	3.7×10^{-6}	512	256	128	>1,024	>4,096	0.25	512	8	4	4	2
N	II	Plasmid	$<10^{-7}$	1.4×10^{-3}	512	256	128	>1,024	32	0.25	512	16	4	64	2
N	II	Plasmid	$<10^{-7}$	5.7×10^{-6}	512	256	128	>1,024	16	8	512	8	4	64	2
N	I	Plasmid (pZB18)	3.1×10^{-4}	7.0×10^{-1}	512	256	2	16	2,048	256	256	64	<0.1	2	2
P	II	Plasmid	$<10^{-7}$	1.7×10^{-5}	512	512	128	>1,024	32	0.25	512	16	8	128	2
P	III	Plasmid	$<10^{-7}$	1.8×10^{-5}	256	64	128	>1,024	64	64	512	16	8	32	2
P	IV	Plasmid	$<10^{-7}$	2.8×10^{-6}	512	16	128	128	32	0.25	512	16	4	64	2
P	II	Plasmid (pZB22)	4.2×10^{-7}	8.5×10^{-3}	512	512	128	>1,024	32	64	512	4	4	64	2
P	II	Plasmid	$<10^{-7}$	2.7×10^{-6}	512	256	128	>1,024	32	0.5	512	16	<0.1	64	2
P	II	Plasmid	$<10^{-7}$	3.1×10^{-6}	512	256	128	>1,024	32	0.25	512	16	<0.1	64	2

and one isolate belonged to ST18 and another to ST25. The remaining five isolates were new STs, designated as ST320, ST335, ST321, ST322, and ST323 (Table 1; http://efaecium.mlst.net/ [accessed 10 February 2007]).

The nearest relation to each of the five new STs was ST80, ST172, ST31, ST262, and ST17, respectively. In total, nine STs (ST323, ST18, ST322, ST25, ST78, ST203, ST320, ST321, and ST335) of the Chinese isolates were categorized into seven clonal complexes (CC), as follows; CC17 (ST323), CC18 (ST18 and ST322), CC25 (ST25), CC78 (ST78 and ST203), CC117 (ST320), CC280 (ST321), and CCS (ST335). Previous reports showed that CC17 strains, which are frequently isolated as hospital outbreak strains, have a genetic lineage to ampicillin resistance and pathogenicity islands containing the *esp* gene (16, 30, 32). The clonal complexes of the Chinese isolates were genetically linked to each other and were close to CC17, except for CCS. All isolates were ampicillin resistant, except for two isolates belonging to CCS and CC25, which were relatively far from the other CCs. Most previously reported hospital outbreak isolates are ampicillin resistant and positive for the *esp* gene (16). However, only 6 of the 11 ampicillin-resistant isolates in this study were found to carry the *esp* gene.

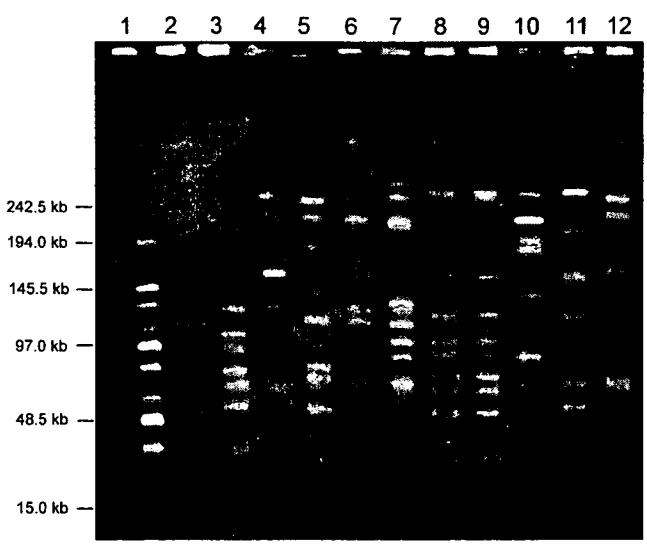

FIG. 1. PFGE of SmaI-digested chromosomal DNAs. Lane 1, molecular mass marker (Midrange Molecular Marker; New England Biolabs); lanes 2 to 12, plasmid DNAs from strains ZB11, ZB14, ZB15, ZB16, ZB22, ZB19, ZB23, ZB24, ZB21, ZB18, and ZB20, respectively.

Analysis of VanA-type vancomycin resistance genes encoded on Tn*1546*-like elements. Since, most Tn*1546*-like elements encoding VanA-type vancomycin resistance are plasmid borne (4), all of the isolates in this study were examined for plasmid content and location of the *vanA* gene by Southern hybridization. The EcoRI restriction profiles of total plasmid DNAs isolated from the VRE strains showed that the plasmids of strain ZB23 were identical to those of strain ZB24 and that the plasmids of strain ZB14 were closely related to those of strain ZB15 (Fig. 2A). Other strains showed heterogeneous plasmid patterns. The *vanA* probe hybridized to an EcoRI fragment in plasmid DNA from each of the strains (Fig. 2B). These results indicated that all of the VanA determinants (Tn*1546*-like elements) were carried on plasmids in these VRE strains. The transferabilities of the vancomycin-resistant traits of the strains were examined by broth mating and filter mating with *E. faecium* BM4105RF used as the recipient strain (Table 1). Vancomycin resistance was transferred at frequencies from 10^{-1} to 10^{-7} per donor cell by filter mating among the strains studied. The vancomycin resistance of ZB18 and ZB22 was transferred at frequencies of 10^{-4} and 10^{-7} per donor cell by broth mating, respectively. All of the vancomycin resistance plasmids were self-transferable or mobile. Two highly conjugative vancomycin resistance plasmids, pZB18 (67 kbp) and pZB22 (200 kbp), were isolated from strains ZB18 and ZB22, respectively (Fig. 3). There are two kinds of highly conjugative plasmids found in enterococci, including pheromone-responsive plasmids of *E. faecalis* and pMG1-like plasmids of *E. faecium* (3, 13). We previously discovered the highly conjugative gentamicin resistance plasmid pMG1 (65 kbp) from an *E. faecium* clinical isolate in Japan (13). pMG1-like plasmids were widely disseminated in vancomycin-resistant *E. faecium* clinical isolates obtained from a hospital in the United States (27). Recently, we also isolated pMG1-like plasmids carrying Tn*1546*-like transposons that encode vancomycin resistance in *E. faecium* clinical isolates in Japan (26, 28). All of the pMG1-like plasmids carry a conserved *traA* gene which is involved in the *tra* gene

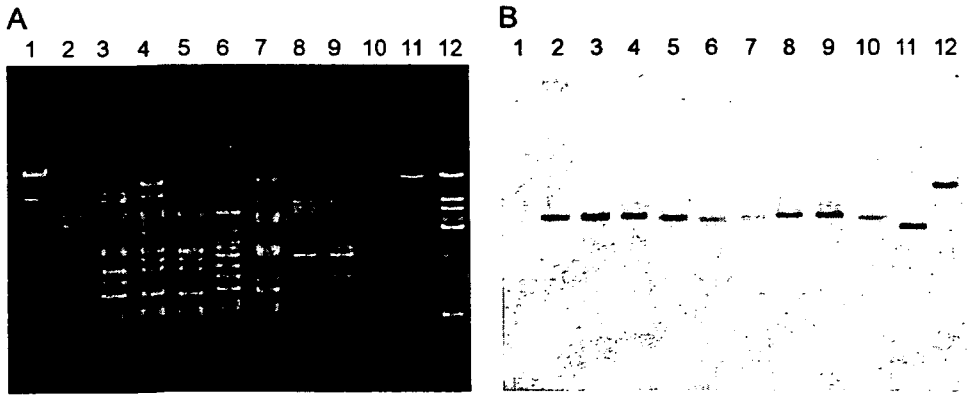

FIG. 2. Agarose gel electrophoresis of EcoRI-digested plasmid DNAs from *E. faecium* isolates (A) and Southern hybridization analysis with the *vanA* probe (B). Lanes 1, HindIII-digested lambda DNA; lanes 2 to 12, plasmid DNAs from strains ZB11, ZB14, ZB15, ZB16, ZB22, ZB19, ZB23, ZB24, ZB21, ZB18, and ZB20, respectively.

system for conjugation and is pMG1 specific (24). pZB18 and pZB22 were examined by PCR amplification to determine whether *traA* was conserved in each of these plasmids. Neither of plasmids carried the *traA* gene. The result implied that both pZB18 and pZB22 were different from the pMG1-like plasmids and could be a new type of highly conjugative *E. faecium* plasmid, as previously reported (23).

The DNA sequences of the Tn*1546*-like elements encoding the *vanA* operon for vancomycin resistance on the plasmids were determined (Fig. 4) (1). Specific primers for the insertion sequences IS*1216V* (809bp) and IS*1542* (1,324bp), which are often found in Tn*1546*-like elements, were used in the sequence analysis (8, 31, 33).

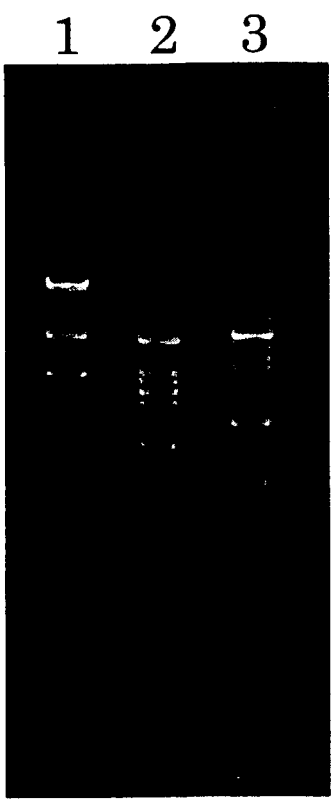

FIG. 3. Agarose gel electrophoresis of the EcoRI-digested highly conjugative plasmid DNA of pZB18 and pZB22. Lane 1, HindIII-digested lambda DNA; lane 2, pZB18; lane 3, pZB22.

A summary of the sequence analysis of the plasmid Tn*1546*-like elements and their comparison to the prototype element (designated type I in this study) are shown in Fig. 4. The *vanS* genes of all of the Chinese isolates were identical to that of the BM4147 strain and had no substitutions. Three specific substitutions within VanS result in low-level teicoplanin resistance, which is frequently found in East Asian VRE isolates (9, 15, 18, 34). The Tn*1546*-like elements of the 13 isolates were classified into six types based on sequence analysis and were designated type I to type VI (Fig. 4). We have reported two VanA-type VRE (*E. faecium*) clinical isolates, C264 and I125, which were originally isolated from patients in China (35). The Tn*1546*-like elements of both strains contained the insertion sequences IS*1216V* and IS*1542* and are classified as type V and type VI, respectively (Fig. 4).

Our group reported the first case of VanA-type *Enterococcus faecalis*: strain KC122.1, isolated in Japan from chicken meat imported from mainland China in 2001 (25). The Tn*1546*-like element was encoded on a conjugative plasmid and had three specific substitutions of VanS, resulting in low-level teicoplanin resistance, as mentioned above. The Tn*1546*-like element of KC122.1 was also examined in this study (Fig. 4). The element was identical to the prototype (type I) except for five point mutations, including the three substitutions within VanS, and had no insertions, suggesting that the origins of the elements of VRE clinical isolates were different from that of the VRE isolate from food animals.

Analytical data for the Tn*1546*-like elements of Chinese VRE isolates can be summarized as follows: (i) all of the elements are plasmid borne; (ii) 12 of the 13 isolates had multiple insertions of IS*1216V* and IS*1542* in the Tn*1546*-like elements; (iii) IS*1542* was inserted into the 8-bp target sequence CTATAATC, from bp 3817 to 3924 of Tn*1546*; (iv) the origins of the two IS*1216V* elements differed from each other, and the IS*1216V* in the *vanXY* region had one base pair substitution (T662C); (v) the distributions and insertions of IS*1216V* and IS*1542* associated with the Tn*1546*-like elements of the Chinese isolates were similar to those previously re-

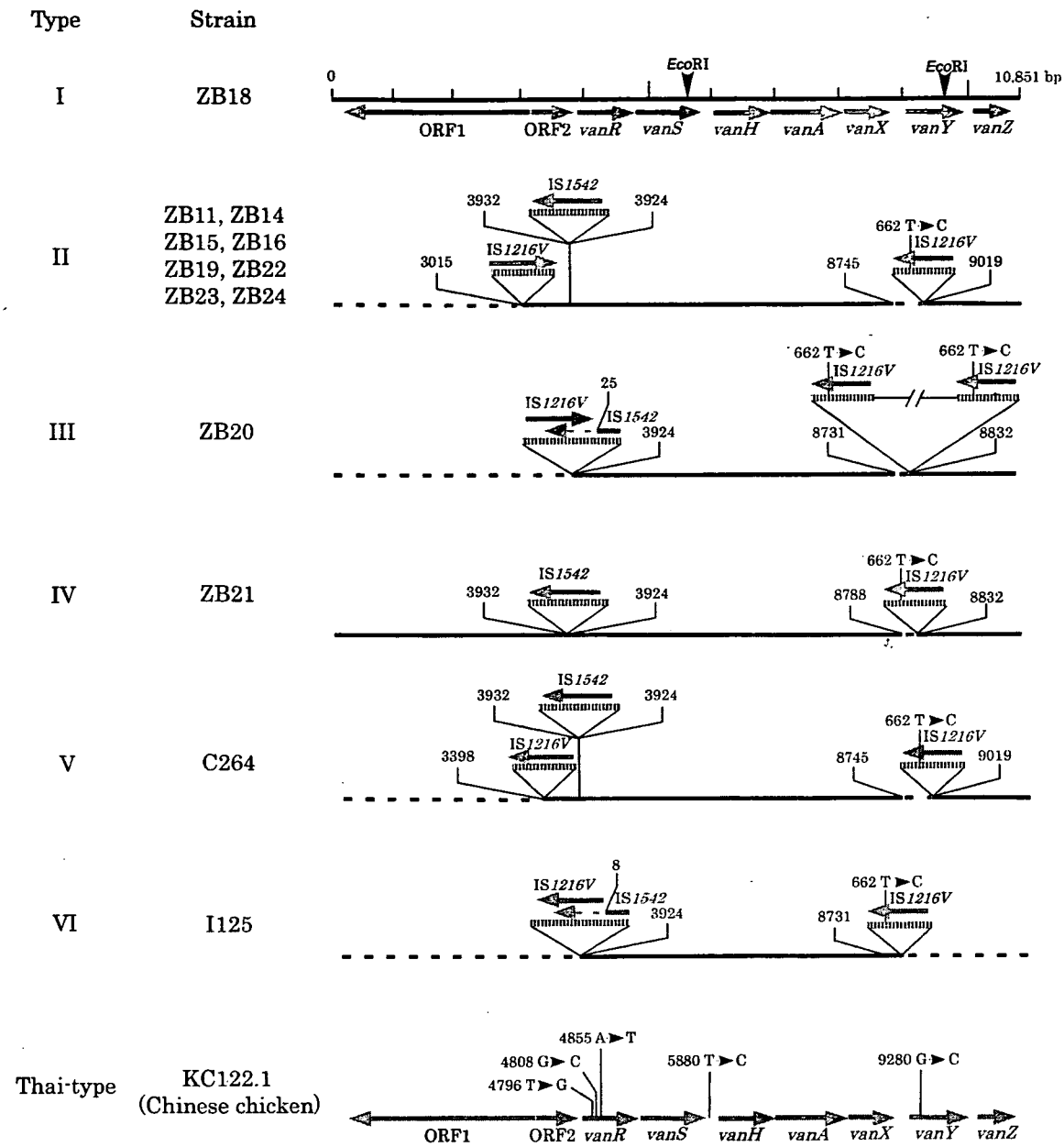

FIG. 4. Genetic organization and typing of Tn*1546*-like elements found in Chinese clinical isolates. The upper horizontal arrows show the genes and open reading frames (ORFs) encoded on the prototype Tn*1546* element of plasmid pIP816 (1). Boxes with vertical lines represent IS elements. The numbers at the IS insertions show the positions of the first nucleotides upstream and downstream of the inserts. The horizontal arrows on the IS elements indicate the transcriptional orientation of the transposase encoded on the ISs. The dotted horizontal lines indicate the deleted region. KC122.1 is a VanA-type *E. faecalis* strain isolated from chicken meat imported from mainland China (25). The Tn*1546*-like element of KC122.1 was temporarily classified as Thai-type, which is often found in VRE isolates from chicken meats imported from Thailand (9, 18).

ported for European and Korean VanA-type VRE isolates (11, 22, 31, 34); (vi) Tn*1546*-like elements were classified into six types, based on DNA sequencing (type I to VI), and type II elements were predominantly isolated from hospitals in Beijing and could be disseminated among different *E. faecium* strains; and (vii) there was no linkage between VRE isolates from humans (patients) and the VRE isolate from a food animal (chicken meat).

This study is the first to provide detailed molecular analyses of VRE clinical isolates from mainland China. To further elucidate the characteristics of Chinese VRE strains, a nationwide surveillance of VRE and systemic analyses of other types of VRE strains are necessary. In the meantime, the current recommended hospital infection control measures for developed countries may be readily implemented to prevent further spread of VRE in mainland China.

ACKNOWLEDGMENTS

This study was supported by grants from the Japanese Ministry of Education, Culture, Sports, Science, and Technology [Tokutei-ryoiki

(Matrix of Infection Phenomena), Kiban (B), Kiban (C)] and the Japanese Ministry of Health, Labor and Welfare (H15-Shinko-9, H18-Shinko-11).

We thank Elizabeth Kamei for revising the manuscript and Takahiro Nomura for technical assistance. We also thank Rob Willems for submission of MLST data.

REFERENCES

1. **Arthur, M., C. Molinas, F. Depardieu, and P. Courvalin.** 1993. Characterization of Tn*1546*, a Tn*3*-related transposon conferring glycopeptide resistance by synthesis of depsipeptide peptidoglycan precursors in *Enterococcus faecium* BM4147. J. Bacteriol. **175**:117–127.
2. **Cetinkaya, Y., P. Falk, and C. G. Mayhall.** 2000. Vancomycin-resistant enterococci. Clin. Microbiol. Rev. **13**:686–707.
3. **Clewell, D. B., and G. M. Dunny.** 2002. Conjugation and genetic exchange in enterococci, p. 359–367. *In* M. S. Gilmore, D. B. Clewell, P. Courvalin, G. M. Dunny, B. E. Murray, and L. B. Rice, (ed.), The enterococci: pathogenesis, molecular biology, and antibiotic resistance. ASM Press, Washington, DC.
4. **Courvalin, P.** 2006. Vancomycin resistance in Gram-positive cocci. Clin. Infect. Dis. **42**:S25–S34.
5. **Dunny, G. M., R. A. Craig, R. L. Carron, and D. B. Clewell.** 1979. Plasmid transfer in *Streptococcus faecalis*: production of multiple sex pheromones by recipients. Plasmid **2**:454–465.
6. **Franke, A., and D. B. Clewell.** 1981. Evidence for a chromosome-borne resistance transposon (Tn*916*) in *Streptococcus faecalis* that is capable of "conjugal" transfer in the absence of a conjugative plasmid. J. Bacteriol. **145**:494–502.
7. **Fujita, N., M. Yoshimura, T. Komori, K. Tanimoto, and Y. Ike.** 1998. First report of the isolation of high-level vancomycin-resistant *Enterococcus faecium* from a patient in Japan. Antimicrob. Agents Chemother. **42**:2150.
8. **Handwerger, S., and J. Skoble.** 1995. Identification of chromosomal mobile element conferring high-level vancomycin resistance in *Enterococcus faecium*. Antimicrob. Agents Chemother. **39**:2446–2453.
9. **Hashimoto, Y., K. Tanimoto, Y. Ozawa, T. Murata, and Y. Ike.** 2000. Amino acid substitutions in the VanS sensor of the VanA-type vancomycin-resistant enterococcus strains result in high-level vancomycin resistance and low-level teicoplanin resistance. FEMS Microbiol. Lett. **185**:247–254.
10. **Homan, W. L., T. David, S. Poznanski, M. Li, G. Hogg, E. Spalburg, J. D. A. Van Embden, and R. J. L. Willems.** 2002. Multilocus sequence typing scheme for *Enterococcus faecium*. J. Clin. Microbiol. **40**:1963–1971.
11. **Huh, J. Y., W. G. Lee, K. Lee, W. S. Shin, and J. H. Yoo.** 2004. Distribution of insertion sequences with Tn*1546*-like elements among *Enterococcus faecium* isolates from patients in Korea. J. Clin. Microbiol. **42**:1897–1902.
12. **Ike, Y., R. A. Craig, B. A. White, Y. Yagi, and D. B. Clewell.** 1983. Modification of *Streptococcus faecalis* sex pheromones after acquisition of plasmid DNA. Proc. Natl. Acad. Sci. USA **8**:5369–5373.
13. **Ike, Y., K. Tanimoto, H. Tomita, K. Takeuchi, and S. Fujimoto.** 1998. Efficient transfer of the pheromone-independent *Enterococcus faecium* plasmid pMG1 (Gm^r) (65.1 kilobases) to *Enterococcus* strains during broth mating. J. Bacteriol. **180**:4884–4892.
14. **Kak, V., and J. W. Chow.** 2002. Acquired antibiotic resistance in enterococci, p. 359–367. *In* M. S. Gilmore, D. B. Clewell, P. Courvalin, G. M. Dunny, B. E. Murray, and L. B. Rice, (ed.), The enterococci: pathogenesis, molecular biology, and antibiotic resistance. ASM Press, Washington, DC.
15. **Lauderdale, T. L., L. C. McDonald, Y. R. Shiau, P. C. Chen, H. Y. Wang, J. F. Lai, and M. Ho.** 2002. Vancomycin-resistant enterococci from humans and retail chickens in Taiwan with unique VanB phenotype-*vanA* genotype incongruence. Antimicrob. Agents Chemother. **46**:525–527.
16. **Leavis, H. L., R. J. L. Willems, J. Top, E. Spalburg, E. M. Mascini, A. C. Fluit, A. Hoepelman, A. J. de Neeling, and M. J. M. Bonten.** 2003. Epidemic and nonepidemic multidrug-resistant *Enterococcus faecium*. Emerg. Infect. Dis. **9**:1108–1115.
17. **Leclercq, R., E. Derlot, J. Duval, and P. Courvalin.** 1988. Plasmid-mediated resistance to vancomycin and teicoplanin in *Enterococcus faecium*. N. Engl. J. Med. **319**:157–161.
18. **Ozawa, Y., K. Tanimoto, T. Nomura, M. Yoshinaga, Y. Arakawam, and Y. Ike.** 2002. Vancomycin-resistant enterococci in humans and imported chickens in Japan. Appl. Environ. Microbiol. **68**:6457–6461.
19. **Palepou, M. F. I., A. M. A. Adebiyi, C. H. Tremlett, L. B. Jensen, and N. Woodford.** 1998. Molecular analysis of diverse elements mediating VanA glycopeptide resistance in enterococci. J. Antimicrob. Chemother. **42**:605–612.
20. **Sahm, D. F., J. Kissinger, M. S. Gilmore, P. R. Murray, R. Mulder, J. Solliday, and B. Clarke.** 1989. In vitro susceptibility studies of vancomycin-resistant *Enterococcus faecalis*. Antimicrob. Agents Chemother. **33**:1588–1591.
21. **Sambrook, J., E. F. Fritsch, and T. Maniatis.** 1989. Molecular cloning: a laboratory manual, 2nd ed. Cold Spring Harbor Laboratory Press, Cold Spring Harbor, NY.
22. **Schouten, M. A., R. J. L. Willems, W. A. G. Kraak, J. Top, J. A. A. Hoogkamp-Korstanje, and A. Voss.** 2001. Molecular analysis of Tn*1546*-like elements in vancomycin-resistant enterococci isolated from patients in Europe shows geographic transposon type clustering. Antimicrob. Agents Chemother. **45**:986–989.
23. **Takeuchi, K., H. Tomita, S. Fujimoto, M. Kudo, H. Kuwano, and Y. Ike.** 2005. Drug resistance of *Enterococcus faecium* clinical isolates and the conjugative transfer of gentamicin and erythromycin resistance traits. FEMS Microbiol. Lett. **243**:347–354.
24. **Tanimoto, K., and Y. Ike.** 2002. Analysis of the conjugal transfer system of the pheromone-independent highly transferable *Enterococcus* plasmid pMG1: identification of a *tra* gene (*traA*) up-regulated during conjugation. J. Bacteriol. **184**:5800–5804.
25. **Tanimoto, K., T. Nomura, H. Hamatani, Y. H. Xiao, and Y. Ike.** 2005. A vancomycin-dependent VanA-type *Enterococcus faecalis* strain isolated in Japan from chickens imported from China. Lett. Appl. Microbiol. **41**:157–162.
26. **Tomita, H., and Y. Ike.** 2005. Genetic analysis of transfer-related regions of the vancomycin resistance *Enterococcus* conjugative plasmid pHTβ: identification of *oriT* and a putative relaxase gene. J. Bacteriol. **187**:7727–7737.
27. **Tomita, H., C. Pierson, S. K. Lim, D. B. Clewell, and Y. Ike.** 2002. Possible connection between a widely disseminated conjugative gentamicin resistance (pMG1-like) plasmid and the emergence of vancomycin resistance in *Enterococcus faecium*. J. Clin. Microbiol. **40**:3326–3333.
28. **Tomita, H., K. Tanimoto, S. Hayakawa, K. Morinaga, K. Ezaki, H. Oshima, and Y. Ike.** 2003. Highly conjugative pMG1-like plasmids carrying Tn*1546*-like transposons that encode vancomycin resistance in *Enterococcus faecium*. J. Bacteriol. **185**:7024–7028.
29. **Uttley, A. H., C. H. Collins, J. Naidoo, and R. C. George.** 1988. Vancomycin-resistant enterococci. Lancet **i**:57–58.
30. **Willems, R. J., W. Homan, J. Top, M. van Santen-Verheuvel, D. Tribe, X. Manzioros, C. Gaillard, C. Vandenbroucke-Grauls, E. Mascini, and E. van Kregten.** 2001. Variant *esp* gene as a marker of a distinct genetic lineage of vancomycin-resistant spreading in hospitals. Lancet **357**:853–855.
31. **Willems, R. J. L., J. Top, N. van den Braak, A. van Belkum, D. J. Mevius, G. Hendriks, M. van Santen-Verheuvel, and J. D. A. van Embden.** 1999. Molecular diversity and evolutionary relationships of Tn*1546*-like elements in enterococci from humans and animals. Antimicrob. Agents Chemother. **43**:483–491.
32. **Willems, R. J. L., J. Top, M. van Santen, D. A. Robinson, T. M. Coque, F. Baquero, H. Grundmann, and M. J. M. Bonten.** 2005. Global spread of vancomycin-resistant *Enterococcus faecium* from a distinct nosocomial genetic complex. Emerg. Infect. Dis. **11**:821–828.
33. **Woodford, N., A. A. Adebiyi, M. I. Palepou, and B. D. Cookson.** 1998. Diversity of VanA glycopeptide resistance elements in enterococci from humans and nonhuman sources. Antimicrob. Agents Chemother. **42**:502–508.
34. **Yu, H. S., S. Y. Seol, and D. T. Cho.** 2003. Diversity of Tn*1546*-like elements in vancomycin-resistant enterococci isolated from humans and poultry in Korea. J. Clin. Microbiol. **41**:2641–2643.
35. **Zheng, B., H. Tomita, Y. H. Xiao, and Y. Ike.** 2007. The first molecular analysis of clinical isolates of VanA-type vancomycin-resistant *Enterococcus faecium* strains in mainland China. Lett. Appl. Microbiol., in press.

Letters in Applied Microbiology ISSN 0266-8254

ORIGINAL ARTICLE

The first molecular analysis of clinical isolates of VanA-type vancomycin-resistant *Enterococcus faecium* strains in Mainland China

B. Zheng[1,2], H. Tomita[2], Y.H. Xiao[1] and Y. Ike[2,3]

1 Institute of Clinical Pharmacology, Peking University First Hospital, Beijing, China
2 Department of Bacteriology and Bacterial Infection Control, Gunma University Graduate School of Medicine, Maebashi, Gunma, Japan
3 Laboratory of Bacterial Drug Resistance, Gunma University Graduate School of Medicine, Maebashi, Gunma, Japan

Keywords
China, *Enterococcus faecium*, insertion sequence, Tn*1546*-like element, VanA-type, vancomycin-resistant *Enterococcus faecium*.

Correspondence
H. Tomita, Department of Bacteriology and Bacterial Infection Control, Gunma University Graduate School of Medicine, Showa-machi 3-39-22, Maebashi, Gunma 371-8511, Japan.
E-mail: tomitaha@med.gunma-u.ac.jp

2006/0256: received 24 February 2006, revised 2 March 2007 and accepted 26 April 2007

doi:10.1111/j.1472-765X.2007.02191.x

Abstract

Aims: The aim of this study was to examine two VanA-type vancomycin-resistant *Enterococcus faecium* (VRE) strains that had been isolated from patients resident in mainland China. This is the first molecular analysis of clinical VRE strains being isolated in mainland China.

Methods and Results: Two VanA-type VRE isolates were isolated from in-patients at hospitals located in the Chinese cities Beijing and Dalian and were designated C264 and I125. The plasmids pC264V (40 kbp) and pI125V (370 kbp) that were isolated from C264 and I125, respectively, carried a Tn*1546*-like element encoding VanA resistance. The vancomycin-resistant plasmids pC264V and pI125V were transferred by filter mating at frequencies of 10^{-7} and 10^{-4} respectively. Sequence analysis of pC264V revealed that two IS*1216V* sequences and an IS*1542* sequence were present within the Tn*1546*-like element. pI125V had two IS*1216V* insertions in the Tn*1546*-like element.

Conclusions: The two VanA-type vancomycin-resistant *E. faecium* (VRE) strains C264 and I125 were isolated from in-patients in Chinese hospitals. The vancomycin-resistant conjugative plasmids pC264V and pI125V plasmids isolated from these strains carried the Tn*1546*-like element. The Tn*1546*-like element was found to contain the insertion sequences IS*1216V* and IS*1542*.

Significance and Impact of the Study: This is the first molecular analysis of VanA-type VRE strains from patients resident in mainland China.

Introduction

The first cases of the isolation of vancomycin-resistant enterococci (VRE) were reported in 1988 in the United Kingdom (Uttley *et al.* 1988) and France (Leclercq *et al.* 1988), and shortly thereafter, VRE was detected in hospitals in the United States (Sahm *et al.* 1989). Since then, VRE have emerged with unanticipated rapidity and are now encountered in many hospitals, particularly in the United States (Martone 1998; Cetinkaya *et al.* 2000).

There have been a number of reports describing the isolation of VRE in East Asian countries such as Japan, Korea and Taiwan. The frequency of VRE isolation from both patients and food animals is increasing in Korea and Taiwan (Kim and Song 1998; Lu *et al.* 2001; Lauderdale *et al.* 2002; Yu *et al.* 2003; Song *et al.* 2005). Japan has also seen an increase in the frequency of VRE isolation from patients (Ike *et al.* 1999; Ozawa *et al.* 2002) since the first report of a VanA-type VRE (*E. faecium*) clinical isolate in 1996 (Fujita *et al.* 1998).

Vancomycin has been used for more than 30 years in China, but to date there has been few reports describing the isolation of clinical VRE strains and no molecular analysis of VRE strains in this country (Wang 2006). We believe this is the first molecular analysis of clinical VanA-type VRE strains in mainland China. In this report,

we describe the molecular analysis of the Tn*1546*-like elements present in the VRE isolates.

Materials and methods

Bacterial strains, media and antibiotics

The vancomycin-resistant *Enterococcus faecium* (VRE) strains C264 and I125 were isolated from in-patients resident at two different hospitals in China in 2001 and 2003 respectively. *Enterococcus faecalis* FA2-2 (Clewell *et al.* 1982), which is rifampicin and fusidic acid resistant, was used as a recipient in the mating experiments. Todd–Hewitt broth (Difco, Detroit, MI, USA) was used as the growth medium for enterococci. Mueller–Hinton (MH) broth and MH agar (Nissui, Tokyo, Japan) were used in the sensitivity assays to test the antibiotic minimal inhibitory concentrations (MICs).

MIC determination

The MICs were determined by the agar dilution method according to the criteria set by the National Committee for Clinical Laboratory Standards (2000) using MH agar.

Mating procedures

Filter mating was performed with a donor/recipient ratio of 1 : 10 (Franke and Clewell 1981). Broth mating was performed as previously described with a donor/recipient ratio of 1 : 10 (Dunny *et al.* 1979). The conjugative transfer frequency was calculated as the ratio of the number of transconjugants to the number of donors.

Isolation and manipulation of plasmid DNA

Plasmid DNA was isolated by the alkaline lysis method (Sambrook *et al.* 1989). Restriction enzymes were obtained from New England Biolabs, Inc. (Beverly, MA, USA) and Takara Bio Inc., (Tokyo, Japan).

DNA sequencing analysis of Tn*1546*-like elements

The DNA fragments to be sequenced were amplified by PCR using the thermostable DNA polymerase TaKaRa *Taq* (Takara Bio Inc.) and a Perkin-Elmer 9600 thermal cycler (Applied Biosystems, Foster City, CA, USA). The PCR conditions were varied according to the primers used and the size of the anticipated product. The custom primers used in this study were obtained from Invitrogen (Tokyo, Japan). The sequencing reaction was carried out with a Dye Terminator Cycle Sequencing FS ready Reaction Kit (Perkin-Elmer). The nucleotide sequence was determined using an ABI PRISM 310 genetic analyser and 377 DNA sequencer (Perkin-Elmer).

Pulsed-field gel electrophoresis

Cells were pretreated with 20 mg ml^{-1} of lysozyme for 2 h and then lysed in an agarose plug according to the standard protocol (Sambrook *et al.* 1989). The agarose plugs were then placed in 300 μl of reaction mixture containing 50 U of *Sma*I to digest total DNA. The gels were electrophoresed with a clamped homogeneous electric field (6 V cm^{-1}, 15°C for 24 h, Switch times ramped from 1 to 25 s; CHEF-DR II; Bio-Rad Laboratories, Richmond, CA, USA).

DNA–DNA Southern hybridization

Southern hybridization was carried out with the digoxigenin-based nonradioisotope system of Boehringer GmbH (Mannheim, Germany), and all procedures were based on the manufacturer's manual and standard protocols (Sambrook *et al.* 1989). The PCR product specific for *vanA* was used to construct a probe for the detection of the *vanA* gene. Signals were detected using nitroblue tetrazolium-5-bromo-4-chloro-3-indolylphosphate stock solution (Roche Diagnostics GmbH, Mannheim, Germany).

Results

Isolation of two VRE strains

The two VRE strains C264 and I125 were isolated from in-patients resident at two different hospitals in 2001 and 2003 respectively. C264 was isolated from bile exudates obtained from a 50-year-old male patient hospitalized in a Beijing hospital who was suffering from progressive gastric cancer with systemic metastasis. The infectious bile exudates were isolated from the percutaneous choledochal drainage tube being used in the treatment of obstructive jaundice caused by the metastasis. Prior to isolation of C264, the patient had been treated with cefoperazone/sulbactam (2·0 g day^{-1} for a total of 32 days), ceftazydime (2·0 g day^{-1} for 4 days) and clindamycin (0·6 g day^{-1} for 3 days). I125 was isolated from sputum obtained from a 45-year-old male patient who had been hospitalized in a Dalian hospital for the treatment of hepatocirrhosis after having undergone a liver transplant. The patient had contracted pneumonia while in the hospital and had been treated with vancomycin (0·5 g day^{-1} for 5 days), cefepime (1·0 g day^{-1} for 3 days) and cefoperazone/sulbactam (2·0 g day^{-1} for 6 days) prior to the isolation of the I125 strain.

Table 1 MICs of the vancomycin-resistant *Enterococcus faecium* isolates ($\mu g \cdot ml^{-1}$)

Drug	C264	I125
Ampicillin	256	64
Imipenem	512	512
Gentamicin	512	512
Erythromycin	512	512
Ofloxacin	64	64
Moxifloxacin	16	8
Gatifloxacin	16	8
Tetracycline	0·5	0·5
Vancomycin	128	32
Teicoplanin	32	32

MIC, minimal inhibitory concentration.

Characterization of the strains

The drug resistance levels (MICs, in $\mu g\ ml^{-1}$) for C264 and I125 are shown in Table 1. C264 has a relatively high-level MIC for vancomycin (128 $\mu g\ ml^{-1}$) and I125 has an intermediate-level MIC for vancomycin (32 $\mu g\ ml^{-1}$). Both isolates have an intermediate level of resistance to teicoplanin (32 $\mu g\ ml^{-1}$ in MIC). The vancomycin resistance genes of the isolates were examined by PCR amplification using specific primers for the reported *van* genes. In both cases, amplified *vanA*-specific products were detected and confirmed by DNA sequencing (data not shown). The pulsed-field gel electrophoresis (PFGE) profiles of *Sma*I-digested chromosomal DNA from C264 and I125 differed from one another and no relationship between the two strains was detected (Fig. 1a).

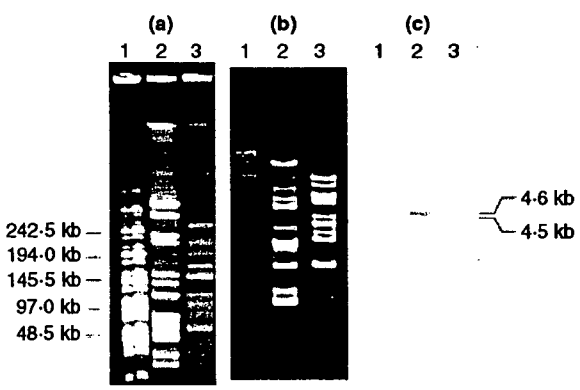

Figure 1 Pulsed-field gel electrophoresis (PFGE) of *Sma*I-digested chromosomal DNAs from vancomycin-resistant *Enterococcus faecium* isolates, C264 and I125 (a). Agarose gel electrophoresis of the *Eco*RI-digested plasmid DNAs from *E. faecium* C264 and I125 isolates (b) and Southern hybridization analysis using *vanA* probe (c). Lane 1: molecular weight markers (a) Midrange PFG marker (New England Biolabs), (b and c) *Hin*dIII-digested lambda DNA; Lane 2: C264; Lane3: I125.

Transferability of vancomycin resistance and the vancomycin-resistant plasmids

The transfer of vancomycin resistance by broth mating and by filter mating was examined in the two VRE isolates. The vancomycin resistances of C264 and I125 only transferred to *E. faecalis* FA2-2 strains by filter mating at frequencies of 10^{-7} and 10^{-4} per donor cell respectively.

*Eco*RI-digested plasmid DNA prepared from C264 and I125 showed that both strains harbored several plasmids (Fig. 1b). The plasmid DNAs were examined by Southern hybridization analysis using the *vanA* probe (Fig. 1c). The *vanA* probe hybridized to a 4·6 kbp *Eco*RI fragment of plasmid DNA obtained from C264 and a 4·5 kbp *Eco*RI fragment of plasmid DNA obtained from I125. The intensity of the 4·5 kbp band of I125 was relatively faint compared with that of the 4·6 kbp band of C264 on the Southern blot membrane (Fig. 1c).

To confirm that the *vanA* gene of I125 was encoded on the plasmid, the vancomycin-resistant transconjugant of *E. faecalis* FA2-2 obtained in the mating experiment with I125 was examined in detail. Plasmid DNA prepared from the transconjugant FA2-2/I125V was too faint to detect clearly on the agarose gel. Undigested total DNA prepared from FA2-2/I125V was separated by PFGE and the gel was then Southern blotted and hybridized with the *vanA* probe (data not shown). A 370 kbp DNA fragment had migrated from the well and was detected on the agarose gel. The DNA band appeared to result from nonspecific digestion of the plasmid, and the *vanA* probe hybridized to this band. These data indicated that the *vanA* gene was encoded on the large conjugative plasmid designated as pI125V (370 kbp). PFGE and Southern hybridization detection of the *vanA* gene were performed using C264 and the results showed that the vancomycin resistance was encoded on a 40 kbp conjugative plasmid designated as pC264V.

Structure of the Tn*1546*-like elements

The DNA sequences of the Tn*1546*-like elements encoding the *vanA*-operon were determined for the vancomycin resistance genes encoded on the plasmid pI125V and pC264V. Overlapping internal fragments of the Tn*1546*-like element carried by each plasmid were amplified using the specific primer sets and each amplified PCR product was sequenced and compared with the reported prototype Tn*1546* element (10 851 bp) carried by pIP816 (34 kbp) of *E. faecium* BM4147 (Fig. 2) (Arthur *et al.* 1993). Specific primers for the insertion sequences IS*1216V* (809 bp) and IS*1542* (1324 bp), which are often found in the Tn*1546*-like element, were also used in sequence analysis (Handwerger and Skoble 1995; Woodford *et al.* 1998).

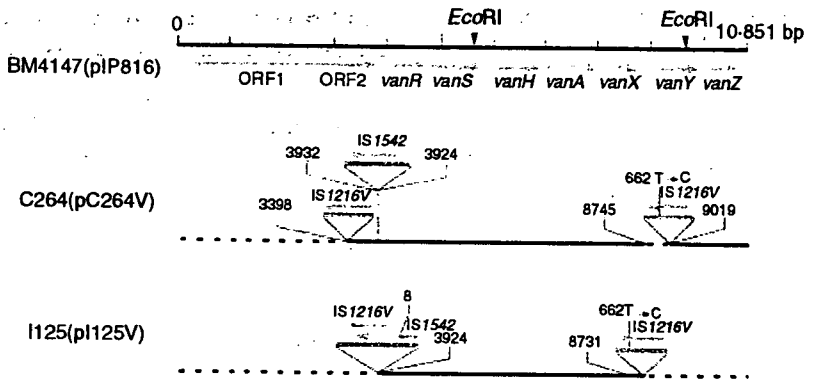

Figure 2 Genetic map and organization of the Tn*1546*-like elements of C264, I125 and the prototype element found in *Enterococcus faecium* BM4147. The upper horizontal arrows show the genes and open reading frames (ORFs) encoded on the prototype Tn*1546* element of plasmid pIP816. Boxes with vertical lines represent insertion sequence (IS) elements. The numbers at the IS insertions show the positions of the first nucleotides upstream and downstream of the inserts. The horizontal arrows on the IS elements indicate the transcriptional orientation of transposase encoded on the ISs. The dotted horizontal lines indicate the deleted region.

The sequence data obtained by analysis of the Tn*1546*-like elements of the plasmids and their comparison with the prototype element are shown in Fig. 2. Sequence analysis of pC264V revealed that the IS*1216V* sequences had inserted into open reading frames 2 (ORF2) upstream of *vanR* and into the internal region between *vanX* and *vanY* of the Tn*1546*-like element of pC264V, and an IS*1542* sequence had inserted into the internal region between ORF2 and the *vanR* gene. IS*1216V* had inserted at 366 bp, and the region upstream of 365 bp in the N-terminal region of ORF2 (576 bp) had been deleted in the Tn*1546*-like element. The deleted region contained ORF1 and the 365 bp N-terminal region of ORF2 of the Tn*1546*-like element. The 273 bp segment upstream of the IS*1216V* insertion within the internal region between *vanX* and *vanY* was also deleted. IS*1542* had inserted at position 3932 bp of Tn*1546* within an 8 bp-duplication that might correspond to the 'CTATAATC' target sequence. pI125V had two IS*1216V* insertions in the Tn*1546*-like element. One IS*1216V* element had inserted at 52 bp in the region upstream of *vanR*. The region upstream of the insertion, where ORF1 and ORF2 were located, had been deleted. Another IS*1216V* had inserted into the internal region between *vanX* and *VanY* and the region downstream of the insertion, where *vanY* and *vanZ* were located, was also deleted. Both plasmids had a nucleotide substitution from T to C at position 662 bp in the IS*1216V* located in the internal region between *vanX* and *vanY* (Fig. 2). The nucleotide substitution did not result in any amino acid substitution in the deduced amino acid sequences of the transposase (228 aa) encoded on IS*1216V*.

Discussion

Vancomycin has been used for about 40 years in the treatment of patients in mainland China, but there has been no report to date describing the isolation of clinical VRE strains. The two VanA-type VRE strains, C264 and I125, are the first clinical isolates of Chinese origin to be reported. The PFGE profiles indicated that they were unrelated, although both carried vancomycin-resistant conjugative plasmids and had insertion sequences in the Tn*1546*-like elements. The *vanS* genes of pC264V and pI125V were identical to that of the BM4147 strain and there were no substitutions in the gene. The resistance levels differed from VanA-type VRE strains that have three substitutions within VanS resulting in low-level teicoplanin resistance, which are frequently isolated in Japan from chicken meat imported from Thailand (Hashimoto *et al.* 2000; Ozawa *et al.* 2002) and are also found in Taiwanese VRE (Lauderdale *et al.* 2002). Recently, a VanA-type *Enterococcus faecalis* strain was isolated from chicken meat imported from China and was described by our group (Tanimoto *et al.* 2005). The isolate harboured the vancomycin-resistance conjugative plasmid and three substitutions within VanS identical to those found in the Thai chicken VRE isolates. Our data showed that the origins of the Chinese clinical VRE isolates differed from that of the VRE isolate obtained from Chinese chicken meat.

Insertion sequences such as IS*1216V* and IS*1542* are frequently found in the Tn*1546*-like elements of VanA-type VRE isolates and partial deletion of DNA is also common (Jensen 1998; Palepou *et al.* 1998; Willems *et al.* 1999; Yu *et al.* 2003). Our sequence analysis showed that

the insertion sequences and deletions were found in the Tn*1546*-like elements of pC264V and pI125V. We were unable to determine why the I125 isolate showed an intermediate level of resistance to vancomycin (MIC; 32 $\mu g\ ml^{-1}$) in this study, but some reports explain the decline in MIC as a result of insertions or deletions within *vanX* and *vanY* , as we had observed in the sequence of pI125V (Lee *et al.* 2004; Naas *et al.* 2005). IS*1542* had inserted at 3932 bp within the pC264V Tn*1546*, within an 8 bp-duplication that might correspond to the 'CTATAATC' target sequence. The target site within the pC264V Tn*1546*-like element was identical to the insertion sites in VanA-type VRE isolates seen in Europe and Korea (Schouten *et al.* 2001; Huh *et al.* 2004; Lee *et al.* 2004). These data imply that the Tn*1546* element has a hot spot sequence for the insertion of IS*1542*. Eight base pair sequences identical to the end of IS*1542* were found between the IS*1216V* sequences and position 3924 bp of Tn*1546* in pI125V, suggesting that IS*1542* had inserted into the Tn*1546* hot spot and then at a later time IS*1216V* had inserted into the IS*1542* (Fig. 2). Both plasmids had a T to C nucleotide substitution at 662 bp in the IS*1216V* in the internal region between *vanX* and *vanY*. The origins of the IS*1216V*s carrying a one base pair substitution might differ from those of the other IS*1216V*s that had no substitution and were located in the upstream region of the Tn*1546*-like element.

Although these VanA-type VRE strains were isolated independently in China, the distribution and insertion of IS*1216V* and IS*1542* associated with the Tn*1546*-like elements of the Chinese isolates were similar to the European and Korean VanA-type VRE isolates that have been previously reported (Willems *et al.* 1999; Darini *et al.* 2000; Schouten *et al.* 2001; Yu *et al.* 2003; Huh *et al.* 2004; Lee *et al.* 2004). In order to understand the characteristics of Chinese VanA-type VRE strains, a nationwide surveillance of VRE would be required as would further analyses of other VanA-type VRE.

Acknowledgements

This study was supported by grants from the Japanese Ministry of Education, Culture, Sport, and Science and Technology [Tokuteiryoiki (C), Kiban (B), Kiban (C)], and the Japanese Ministry of Health, Labor and Welfare (H15-Shinko-9). We thank Dr. Elizabeth Kamei for revising the manuscript.

References

Arthur, M., Molinas, C., Depardieu, F. and Courvalin, P. (1993) Characterization of Tn*1546*, a Tn*3*-related transposon conferring glycopeptide resistance by synthesis of depsipeptide peptidoglycan precursors in *Enterococcus faecium* BM*4147*. *J Bacteriol* **175**, 117–127.

Cetinkaya, Y., Falk, P. and Mayhall, C.G. (2000) Vancomycin-resistant enterococci. *Clin Microbiol Rev* **13**, 686–707.

Clewell, D., Tomich, P., Gawron-Bruke, M., Franke, A.E., Yagi, A. and An, F. (1982) Mapping of *Streptococcus faecalis* plasmids pAD1 and pAD2 and studies relating to transposition of Tn*917*. *J Bacteriol* **152**, 1220–1230.

Darini, A.L., Palepou, M.F. and Woodford, N. (2000) Effects of the movement of insertion sequences on the structure of VanA glycopeptide resistance elements in *Enterococcus faecium*. *Antimicrob Agents Chemother* **44**, 1362–1364.

Dunny, G.M., Craig, R.A., Carron, R.L. and Clewell, D.B. (1979) Plasmid transfer in *Streptococcus faecalis*: production of multiple sex pheromones by recipients. *Plasmid* **2**, 454–465.

Franke, A.E. and Clewell, D.B. (1981) Evidence for a chromosome-borne resistance transposon (Tn*916*) in *Streptococcus faecalis* that is capable of "conjugal" transfer in the absence of a conjugative plasmid. *J Bacteriol* **145**, 494–502.

Fujita, N., Yoshimura, M., Komori, T., Tanimoto, K. and Ike, Y. (1998) First report of the isolation of high-level vancomycin-resistant *Enterococcus faecium* from a patient in Japan. *Antimicrob Agents Chemother* **42**, 2150.

Handwerger, S. and Skoble, J. (1995) Identification of chromosomal mobile element conferring high-level vancomycin resistance in *Enterococcus facium*. *Antimicrob Agents Chemother* **39**, 2446–2453.

Hashimoto, Y., Tanimoto, K., Ozawa, Y., Murata, T. and Ike, Y. (2000) Amino acid substitutions in the VanS sensor of the VanA-type vancomycin-resistant *Enterococcus* strains results in high-level vancomycin resistance and low-level teicoplanin resistance. *FEMS Microbiol Lett* **185**, 247–254.

Huh, J.Y., Lee, W.G., Lee, K., Shin, W.S. and Yoo, J.H. (2004) Distribution of insertion sequences associated with Tn*1546*-like elements among *Enterococcus faecium* isolates from patients in Korea. *J Clin Microbiol* **42**, 1897–1902.

Ike, Y., Tanimoto, K., Ozawa, Y., Nomura, T., Fujimoto, S. and Tomita, H. (1999) Vancomycin-resistant enterococci in imported chickens in Japan. *Lancet* **353**, 1854.

Jensen, L.B. (1998) Internal size variations in Tn*1546*-like elements due to the presence of IS*1216V*. *FEMS Microbiol Lett* **169**, 349–354.

Kim, J.M. and Song, Y.G. (1998) Vancomycin-resistant enterococcal infections in Korea. *Yonsei Med J* **39**, 562–568.

Lauderdale, T.L., McDonald, L.C., Shiau, Y.R., Chen, P.C., Wang, H.Y., Lai, J.F. and Ho, M. (2002) Vancomycin-resistant enterococci from humans and retail chickens in Taiwan with unique VanB phenotype-*vanA* genotype incongruence. *Antimicrob Agents Chemother* **46**, 525–527.

Leclercq, R., Derlot, E., Duval, J. and Courvalin, P. (1988) Plasmid-mediated resistance to vancomycin and teicoplanin in *Enterococcus faecium*. *N Engl J Med* **319**, 157–161.

Lee, W.G., Hun, J.Y., Cho, S.R. and Lim, Y.A. (2004) Reduction in glycopeptide resistance in vancomycin-resistant

enterococci as a result of *vanA* cluster rearrangements. *Antimicrob Agents Chemother* **48**, 1379–1381.

Lu, J.J., Perng, C.L., Chiueh, T.S., Lee, S.Y., Chen, C.H., Chang, F.Y., Wang, C.C. and Chi, W.M. (2001) Detection and typing of vancomycin-resistance genes of enterococci from clinical and nosocomial surveillance specimens by multiplex PCR. *Epidemiol Infect* **126**, 357–363.

Martone, W.J. (1998) Spread of vancomycin resistant enterococci: why did it happen in the United States? *Infect Control Hosp Epidemiol* **19**, 539–545.

Naas, T., Fortineau, N., Snanoudj, R., Spicq, C., Durrbach, A. and Nordmann, P. (2005) First nosocomial outbreak of vancomycin-resistant *Enterococcus feacium* expressing a VanD-like phenotype associated with vanA genotype. *J Clin Microbiol* **43**, 3642–3649.

Ozawa, Y., Tanimoto, K., Nomura, T., Yoshinaga, M., Arakawa, Y. and Ike, Y. (2002) Vancomycin-resistant enterococci in humans and imported chickens in Japan. *Appl Environ Microbiol* **68**, 6457–6461.

Palepou, M.F., Adebiyi, A.M., Tremlett, C.H., Jensen, L.B. and Woodford, N. (1998) Molecular analysis of diverse elements mediating VanA glycopeptide resistance in enterococci. *J Antimicrob Chemother* **42**, 605–612.

Sahm, D.F., Kissinger, J., Gilmore, M.S., Murray, P.R., Mulder, R., Solliday, J. and Clarke, B. (1989) *In vitro* susceptibility studies of vancomycin-resistant *Enterococcus faecalis*. *Antimicrob Agents Chemother* **33**, 1588–1591.

Sambrook, J., Fritsch, E.F. and Maniatis, T. (1989) *Molecular Cloning: A Laboratory Manual*, 2nd edn. Cold Spring Harbor, NY: Cold Spring Harbor Laboratory Press.

Schouten, M.A., Willems, R.J., Kraak, W.A., Top, J., Hoogkamp-Korstanje, J.A. and Voss, A. (2001) Molecular analysis of Tn*1546*-like elements in vancomycin-resistant enterococci isolated from patients in Europe shows geographic transposon type clustering. *Antimicrob Agents Chemother* **45**, 986–989.

Song, J.Y., Hwang, I.S., Eom, J.S., Cheong, H.J., Bae, W.K., Park, Y.H. and Kim, W.J. (2005) Prevalence and molecular epidemiology of vancomycin-resistant enterococci (VRE) strains isolated from animals and humans in Korea. *Korean J Intern Med* **20**, 55–62.

Tanimoto, K., Nomura, T., Hamatani, H., Xiao, Y.H. and Ike, Y. (2005) A vancomycin-dependent VanA-type *Enterococcus faecalis* strain isolated in Japan from chicken imported from China. *Lett Appl Microbiol* **41**, 157–162.

Uttley, A.H., Collins, C.H., Naidoo, J. and George, R.C. (1988) Vancomycin-resistant enterococci. *Lancet* **1**, 57–58.

Wang, F. (2006) CHINET 2005 surveillance of bacterial resistance in China. *Chinese J Infect Chemother* **6**, 289–295.

Willems, R.J., Top, J., van den Braak, N., van Belkum, A., Mevius, D.J., Hendriks, G., van Santen-Verheuvel, M. and van Embden, J.D. (1999) Molecular diversity and evolutionary relationships of Tn*1546*-like elements in enterococci from humans and animals. *Antimicrob Agents Chemother* **43**, 483–491.

Woodford, N., Anebiyi, A.M., Palepou, M.F. and Cookson, B.D. (1998) Diversity of VanA glycopeptide resistance elements in enterococci from humans and nonhuman sources. *Antimicrob Agents Chemother* **42**, 502–508.

Yu, H.S., Seol, S.Y. and Cho, D.T. (2003) Diversity of Tn*1546*-like elements in vancomycin-resistant enterococci isolated from humans and poultry in Korea. *J Clin Microbiol* **41**, 2641–2643.

JOURNAL OF BACTERIOLOGY, Mar. 2008, p. 2075–2085 Vol. 190, No. 6
0021-9193/08/$08.00+0 doi:10.1128/JB.01056-07

Cloning and Genetic Analyses of the Bacteriocin 41 Determinant Encoded on the *Enterococcus faecalis* Pheromone-Responsive Conjugative Plasmid pYI14: a Novel Bacteriocin Complemented by Two Extracellular Components (Lysin and Activator)▽†

Haruyoshi Tomita,[1] Elizabeth Kamei,[1] and Yasuyoshi Ike[1,2]*

Department of Bacteriology and Bacterial Infection Control[1] and Laboratory of Bacterial Drug Resistance,[2] Gunma University Graduate School of Medicine, Maebashi, Gunma, Japan

Received 5 July 2007/Accepted 4 January 2008

The conjugative plasmid pYI14 (61 kbp) was isolated from *Enterococcus faecalis* YI714, a clinical isolate. pYI14 conferred a pheromone response on its host and encoded bacteriocin 41 (*bac41*). Bacteriocin 41 (Bac41) only showed activity against *E. faecalis*. Physical mapping of pYI14 showed that it consisted of EcoRI fragments A to P. The clone pHT1100, containing EcoRI fragments A (12.6 kbp) and H (3.5 kbp), conferred the bacteriocin activity on *E. faecalis* strains. Genetic analysis showed that the determinant was located in a 6.6-kbp region within the EcoRI AH fragments. Six open reading frames (ORFs) were identified in this region and designated ORF7 (*bacL*$_1$) ORF8 (*bacL*$_2$), ORF9, ORF10, ORF11 (*bacA*), and ORF12 (*bacI*). They were aligned in this order and oriented in the same direction. ORFs *bacL*$_1$, *bacL*$_2$, *bacA*, and *bacI* were essential for expression of the bacteriocin in *E. faecalis*. Extracellular complementation of bacteriocin expression was possible for *bacL*$_1$ and -*L*$_2$ and *bacA* mutants. *bacL*$_1$ and -*L*$_2$ and *bacA* encoded bacteriocin component L and activator component A, respectively. The products of these genes are secreted into the culture medium and extracellularly complement bacteriocin expression. *bacI* encoded immunity, providing the host with resistance to its own bacteriocin activity. The *bacL*$_1$-encoded protein had significant homology with lytic enzymes that attack the gram-positive bacterial cell wall. Sequence data for the deduced *bacL*$_1$-encoded protein suggested that it has a domain structure consisting of an N-terminal signal peptide, a second domain with the enzymatic activity, and a third domain with a three-repeat structure directing the proenzyme to its cell surface receptor.

Bacteriocins are bacterial proteins or peptides which inhibit the growth of other bacteria that are closely related to the producer strain. They usually exhibit a relatively narrow spectrum of activity and are produced by a wide variety of gram-positive and gram-negative bacteria (27). Bacteriocin production is thought to provide the host strain with an ecological or other selective advantage over other strains.

Many *Enterococcus faecalis* clinical isolates produce a bacteriocin (3, 5), and the bacteriocin is frequently encoded on the *E. faecalis* pheromone-responding conjugative plasmid (6, 14, 21, 46). Several *E. faecalis* bacteriocins have been genetically and biochemically characterized (15, 35), including the β-hemolysin/bacteriocin (cytolysin) (6, 7, 18, 20, 22) and the peptide antibiotics AS-48 (33), bacteriocin 21 (47), and bacteriocin 31 (46), which are encoded by the *E. faecalis* conjugative plasmids pAD1 (58 kbp), pMB2 (58 kbp), pPD1 (59 kbp), and pYI17 (57.5 kbp), respectively.

A significant number of *E. faecalis* clinical isolates produce hemolysin/bacteriocin (10, 26), and more than 50% of the hemolytic clinical isolates carry transferable hemolysin/bacteriocin determinants (21, 26). The hemolysin/bacteriocin of pAD1 is associated with virulence in animal models (4, 25, 29), and this plasmid is considered to be a typical *E. faecalis* hemolysin/bacteriocin plasmid (21, 31). The mechanism of hemolysin/bacteriocin production in *E. faecalis* has been studied in detail with the hemolysin/bacteriocin determinant on this plasmid (16, 17, 18, 22, 39). The active hemolysin/bacteriocin is produced by extracellular complementation of the two CylL factors (i.e., $CylL_L$ and $cylL_S$) and CylA.

Previously, we have shown that bacteriocins or bacteriocinogenic *E. faecalis* clinical isolates can be classified into five groups on the basis of their bacteriocin activity against *E. faecalis* FA2-2 and OG1-10, *Enterococcus hirae* 9790, *Streptococcus pyogenes*, *Streptococcus agalactiae*, *Streptococcus sanguinis*, *Streptococcus pneumoniae*, *Staphylococcus aureus*, and *Staphylococcus epidermidis* (46). *E. faecalis* FA-2-2 and OG1-10 and *E. hirae* have been chosen as representative enterococcal strains for the examination and classification of the bacteriocins produced by the clinical isolates in this study. Class 1 types produce the β-hemolysin/bacteriocin (cytolysin) and are active against a wide variety of gram-positive bacteria, including *S. aureus* (2, 15, 17, 24, 46). The β-hemolysin/bacteriocin (cytolysin) of pAD1 belongs to class 1. Class 2 is active against a broad spectrum of bacteria, including *E. faecalis*, other *Streptococcus* spp., and *S. aureus*. AS-48 and bacteriocin 21 belong to class 2. Class 3 is active against *E. faecalis* and *E. hirae*. Class 4 is active against *E. faecalis*, and class 5 is active against *E. hirae*. The YI717, YI718, and YI719 strains belong to class 3 and harbor plasmids pYI17 (57.5 kb), pYI18,

* Corresponding author. Mailing address: Department of Bacteriology and Bacterial Infection Control, Gunma University Graduate School of Medicine, Showa-machi 3-39-22, Maebashi, Gunma 371-8511, Japan. Phone: 81-27-220-7990. Fax: 81-27-220-7996. E-mail: yasuike@med.gunma-u.ac.jp.

† Supplemental material for this article may be found at http://jb.asm.org/.

▽ Published ahead of print on 18 January 2008.